iScience

Article

Drosophila peptidyl-prolyl *cis/trans* isomerase-like 4 regulates circadian rhythm by supporting high-amplitude oscillations of PERIOD

Graphical abstract

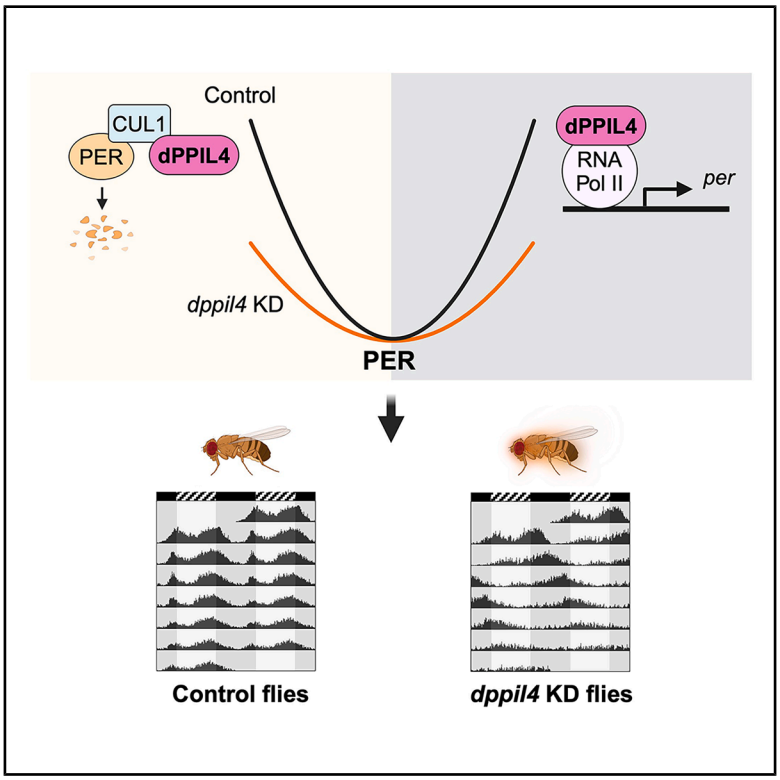

Highlights

- PPIase *dppil4* knockdown lengthens the circadian period in *Drosophila*
- dPPIL4 enhances PER expression via RNA pol II CTD Ser5 phosphorylation
- dPPIL4 stabilizes CUL1 of SCF complex to facilitate timely PER degradation
- dPPIL4 ensures high-amplitude PER oscillation for robust circadian rhythms

Authors

So Who Kang, Hong Thuan Tran, Gaeun Lee, Jestlin Tianthing Ng, Su Bin Lim, Eun Young Kim

Correspondence

ekim@ajou.ac.kr

In brief

Natural sciences; Biological sciences; Neuroscience; Behavioral neuroscience; Molecular neuroscience

Kang et al., 2025, iScience *28*, 112457
May 16, 2025
https://doi.org/10.1016/j.isci.2025.112457

CellPress

iScience

CellPress
OPEN ACCESS

Article

Drosophila peptidyl-prolyl *cis/trans* isomerase-like 4 regulates circadian rhythm by supporting high-amplitude oscillations of PERIOD

So Who Kang,[1,2] Hong Thuan Tran,[1,2,4] Gaeun Lee,[1,2] Jestlin Tianthing Ng,[3] Su Bin Lim,[3] and Eun Young Kim[1,2,5,*]

[1]Department of Biomedical Sciences, Ajou University Graduate School of Medicine, 164 Worldcup-ro, Suwon, Kyunggi-do 16499, Republic of Korea

[2]Department of Brain Science, Ajou University School of Medicine, 164 Worldcup-ro, Suwon, Kyunggi-do 16499, Republic of Korea

[3]Department of Biochemistry, Ajou University School of Medicine, 164 Worldcup-ro, Suwon, Kyunggi-do 16499, Republic of Korea

[4]Present address: Stem Cell Institute, University of Science, Vietnam National University, Ho Chi Minh City, Vietnam

[5]Lead contact

*Correspondence: ekim@ajou.ac.kr

https://doi.org/10.1016/j.isci.2025.112457

SUMMARY

Peptidyl-prolyl *cis/trans* isomerases (PPIases) accelerate proline peptide bond isomerization, affecting substrate protein function. In this study, through RNAi-based behavioral screening of PPIases in *Drosophila melanogaster*, we identified *CG5808*, termed *Drosophila* peptidyl-prolyl *cis/trans* isomerase-like 4 (dPPIL4), as crucial for circadian rhythm regulation. Knockdown of *dppil4* in clock cells lengthened the circadian rhythm period and decreased rhythmicity, accompanied by a significant reduction of core clock protein PERIOD (PER). *dppil4* knockdown downregulated *per* transcription and reduced phosphorylation at Ser5 in the RNA polymerase II C-terminal domain, critical for transcription elongation. In addition, dPPIL4 stabilized Cullin1 of the Skp1-Cullin1-F-box protein complex, a key regulator of PER degradation. Our findings suggest that dPPIL4 supports high-amplitude PER oscillation by enhancing both synthesis and degradation processes in a timely manner. In conclusion, our study underscores the importance of high-amplitude PER oscillations in PER for robust circadian rhythms and highlights the critical role of dPPIL4 in this process.

INTRODUCTION

The circadian timing system enables organisms to manifest circadian (approximately 24-h) rhythmic physiology and behavior, synchronized with environmental cycles such as light/dark and temperature fluctuations.[1] At the molecular and cellular levels, the circadian rhythms are governed by transcriptional-translational feedback loops (TTFLs) involving core clock proteins. While specific proteins may vary, the underlying mechanism is conserved across species.[2,3] In the core TTFL of *Drosophila*, the transcription factors CLOCK (CLK) and CYCLE (CYC) activate the transcription of the *period* (*per*) and *timeless* (*tim*) genes. The translated PER and TIM proteins then repress CLK/CYC, inhibiting their own expression.[4,5] In the secondary loop, CLK/CYC activates the transcription of *vrille* (*vri*) and PAR-domain protein 1ε (*pdp1ε*). VRI and PDP1ε repress and activate *Clk* transcription, respectively, to stabilize the TTFL.[6,7] Additionally, in the tertiary loop, *clockwork orange* is rhythmically expressed by CLK/CYC and modulate its activity.[8–11]

In addition to the transcriptional control, posttranslational modifications (PTMs) of clock proteins are crucial for generating precise circadian rhythm. Particularly, time-dependent interactions of PTMs, including phosphorylation and ubiquitination, determine the proper rhythms of PER abundance, driving the molecular clock's pace. PER is progressively phosphorylated throughout the day by kinases such as DOUBLE TIME and NEMO.[12–14] Ultimately, PER phosphorylation at Ser47 is recognized by supernumerary limbs (Slimb), a component of the Skp1-Cullin1-F-box (SCF) ubiquitin ligase complex, leading to PER degradation and cycle termination.[15–17]

Peptidyl-Prolyl *cis/trans* isomerases (PPIases) accelerate *cis/trans* isomerization of proline peptide bond,[18] a naturally slow process. PPIases categorized into cyclophilin,[19] FK506-binding proteins (FKBPs),[20] Parvulin,[21] and Ser/Thr phosphatase 2A activators (PTPAs),[22] facilitate nascent protein folding and induce conformational changes in mature proteins, impacting their functions. Acting as molecular switches, PPIases alter the fate of substrate proteins and significantly impact several cellular processes such as transcription, ion channel gating, protein degradation, PTM, and enzymatic activity.[23,24] Consequently, dysfunctions in PPIases are associated with various human diseases, including neurodegenerative disease,[25] cancer,[26,27] cardiovascular disease,[28] and viral infection.[29,30]

Given the broad involvement of PPIases in cellular processes, we hypothesized that they might also influence the circadian timing system. In a previous study, we found that *dodo* (*dod*), a homolog of mammalian PPIase Pin1, affected the circadian period length by interacting with hyper-phosphorylated PER

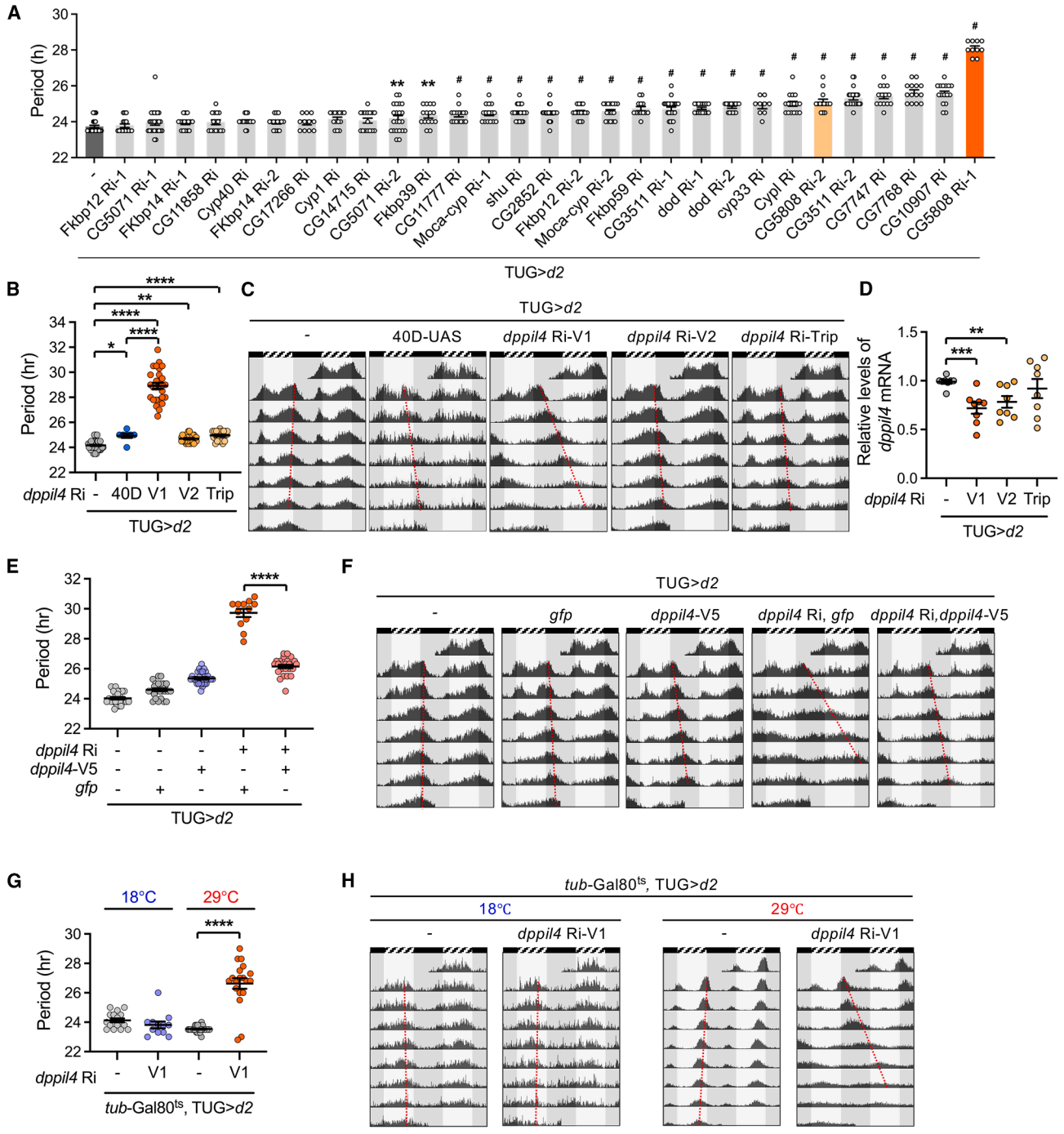

Figure 1. Downregulation of *dppil4* in clock cells lengthened the free-running period

(A) w^{1118} (*w*) or UAS-*ppiase* RNAi flies were crossed with UAS-*dicer2*;*tim*(UAS)-Gal4 (TUG>*d2*) flies. Flies were entrained with a 12:12-h light-dark cycle (LD) for 4 days and maintained in a constant dark (DD) condition at 25°C. The locomotor activity rhythms of flies analyzed in the DD and free-running periods are shown. Values indicate the mean ± SEM. Statistically significant differences between control and KD flies were analyzed using one-way ANOVA followed by Dunnett's multiple comparisons test (**$p < 0.01$, #$p < 0.0001$, n = 11–31). See Table S1 for additional details of behavior analysis.

(B) Three independent *dppil4* RNAi lines were crossed with TUG>*d2* flies, and their locomotor activity rhythms were analyzed. The free-running periods are shown. Please denote that all three KD fly lines showed a long period. 40D: 40D-UAS (VDRC60101); V1: VDRC103789; V2: VDRC22199, and Trip: BDSC55208. Values indicate the mean ± SEM. Statistically significant differences between control and KD flies were analyzed by one-way ANOVA followed by Dunnett's multiple comparisons test (*$p < 0.05$, **$p < 0.01$, ****$p < 0.0001$, n = 7–56). See Table S2 for additional details of behavior analysis.

(legend continued on next page)

and affecting its stability in *Drosophila*.[31] In mammals, cyclophilin-type PPIases catalyze the conformational change of Proline625 in BMAL1, a circadian transcription factor, within its transactivation domain region. Inhibition of this isomerization by cyclosporin A, a cyclophilin blocker, lengthened the circadian period.[32] Motivated by these findings, we conducted targeted RNAi-based behavioral screening by knocking down PPIases in clock cells and analyzing the circadian rhythm behavior. We discovered that *CG5808* (*dppil4*) is required to maintain a 24-h circadian rhythm period. Knockdown (KD) of *dppil4* lengthened the circadian rhythm period to 29 h and significantly reduced PER levels in clock neurons. We further revealed that dPPIL4 modulates *per* RNA transcription by regulating the phosphorylation status of the RNA polymerase II (RNAPII) C-terminal domain (CTD). Additionally, dPPIL4 stabilizes Cullin1 (CUL1) of the SCF complex, a key regulator controlling PER degradation. Overall, dPPIL4 is required to set the circadian rhythm period by supporting high-amplitude PER oscillations.

RESULTS

Downregulation of *dppil4* in clock cells lengthens the free-running period

To investigate whether PPIases are involved in circadian rhythm regulation, we conducted behavioral RNAi screening using the Gal4-UAS system (Table S1). The *Drosophila* genome contains 23 annotated PPIase genes. We crossed each PPIase RNAi line with the *tim*(UAS)-Gal4 (TUG) driver. Most PPIase knockdown (KD) flies exhibited a lengthened period compared to control flies (Figure 1A). Specifically, downregulation of *CG5808* lengthened the period by 0.6 h (V2 line) and 4.8 h (V1 line). Another *CG5808* KD fly line produced using Trip RNAi also showed a long period (Figures 1B and 1C; Table S2). Since the V1 RNAi line is inserted at the 40D locus, causing ectopic overexpression of *tiptop* (*tio*) gene, we analyzed TUG driven 40D-UAS control flies to determine if the long-period phenotype was due to *tio* overexpression.[33,34] Although *tio* overexpression slightly lengthened the circadian period, the effect was not pronounced as the period extension observed in CG5808 KD flies. Therefore, we concluded that the long-period phenotype in CG5808 KD flies expressing V1 line is primarily due to CG5808 KD and not *tio* overexpression. This long-period phenotype was previously noted in a study screening circadian rhythm-related RNA binding protein,[35] but the role of CG5808 in the circadian clock had not been mechanistically investigated. Daily locomotor activity profiles under light-dark (LD) conditions showed that V1 line *CG5808* KD flies exhibited reduced morning anticipation, and a delayed evening activity peak compared to two control lines, TUG>*d2* and TUG>*d2*, UAS-40D (Figure S1). Similarly, *CG5808* KD flies expressing the V2 line showed reduced morning anticipation, while those expressing the Trip line exhibited reduced morning anticipation and a slightly delayed evening activity peak, consistent with their lengthened circadian period (Figure S1).

The *Drosophila CG5808* gene is an ortholog of mammalian PPIL4, hence we termed *CG5808* as *Drosophila* PPIL4 (dPPIL4). *dppil4* mRNA levels were reduced in all three KD lines, although the Trip line reduction was not statistically significant (Figure 1D). Consistent with the period-lengthening effect, the V1 line showed the most significant mRNA decrease (Figure 1D). To confirm that *dppil4* downregulation caused the long period, we expressed *dppil4* in the *dppil4* KD background using the TUG driver. While TUG-driven *dppil4* overexpression lengthened the period by approximately 1 h, *dppil4* overexpression restored the long period induced by *dppil4* KD, indicating that *dppil4* is an on-target of RNAi and is responsible for the long-period phenotype (Figures 1E and 1F; Table S2).

To confirm the role of *dppil4* for circadian function, we generated *dppil4* loss-of-function mutant flies by imprecise excision of the P element inserted in the P{EY13836} fly line. Three lines of deletion mutants were obtained and designated as $dppil4^{ex81}$, $dppil4^{ex88}$, and $dppil4^{ex170}$ (Figure S2A). Genomic DNA PCR and sequencing confirmed the deleted regions of the chromosome (Figure S2B). Unfortunately, flies carrying null alleles were unable to survive to adulthood, indicating that the *dppil4* gene is essential for development. Consequently, we performed behavioral analysis using $dppil4^{ex88}$ heterozygote flies and precisely excised control flies. Heterozygous $dppil4^{ex88}$ flies exhibited normal circadian period and rhythmicity, suggesting that a single functional copy of *dppil4* is sufficient to maintain its role in regulating circadian rhythm (Figure S2). Next, to address potential developmental effects of *dppil4* KD on the circadian phenotype, we employed a temporal and regional gene expression targeting (TARGET) system to restrict KD until behavioral analysis. At 18°C, where temperature-sensitive GAL80 inhibits GAL4 activity, the circadian period was comparable between control and *dppil4* RNAi lines. However, at 29°C, the restrictive temperature where GAL80 inhibition is relieved, the circadian period was significantly lengthened in RNAi lines compared to controls (Figures 1G and 1H; Table S2). This demonstrates that *dppil4* KD during adulthood is sufficient to lengthen the circadian period, which negates the developmental

(C, F, and H) Actograms of flies during seven consecutive days of the DD condition after 4 days of LD entrainment. Actograms are double-plotted to better visualize the rhythmic behavior. Hatched horizontal bars represent subjective day, and black horizontal bars represent subjective night. The dotted red lines connect the evening peaks for each day of the experiment. n = 29–56 for (C), n = 30–32 for (F), and n = 30–32 for (H).

(D) The *dppil4* mRNA levels were quantified in control (TUG>*d2*) and *dppil4* KD (TUG>*d2*, *dppil4* Ri-V1 or V2 or Trip) flies' head using real-time qRT-PCR. Values indicate the mean ± SEM. Statistically significant differences were analyzed using Mann-Whitney test (**$p < 0.01$, ***$p < 0.001$, n = 8).

(E) w^{1118}, UAS-*dppil4* Ri, UAS-*dppil4*, or UAS-*gfp* flies crossed with TUG>*d2* flies singly or in combination as shown on the bottom. Values indicate the mean ± SEM. Statistically significant differences were analyzed with one-way ANOVA followed by Sidak's multiple comparisons test (****$p < 0.0001$, n = 12–32). See Table S2 for additional details of behavior analysis.

(G) *dppil4* was downregulated in an adult-specific manner using the TARGET system. Flies were reared at 18°C, and the locomotor activity rhythms of adult flies were analyzed at 18°C and 29°C. Please denote that the locomotor activity period was normal at 18°C, when $Gal80^{ts}$ inhibited Gal4 activity, but was lengthened at 29°C when *dppil4* was downregulated. Values indicate the mean ± SEM. Statistically significant differences were analyzed using one-way ANOVA followed by Sidak's multiple comparisons test (****$p < 0.0001$, n = 26–32). See Table S2 for additional details of behavior analysis.

role of dPPIL4. Collectively, these results clearly indicate that dPPIL4 is required in clock cells to regulate the circadian period.

dPPIL4 is broadly expressed in brain cells, including clock neurons, and is localized in the nucleus

We examined whether *dppil4* expression is rhythmic under the LD cycle. *dppil4* mRNA levels were constant throughout the day in control flies, indicating that *dppil4* expression is not regulated by the circadian clock. In *dppil4* KD flies, we confirmed a reduction in *dppil4* mRNA levels (Figure 2A). Similarly, dPPIL4 protein abundance was constant throughout the day, and significantly reduced in *dppil4* KD flies (Figures 2B and 2C; Figure S3).

Next, to assess the involvement of dPPIL4 within circadian clock neuronal network, we performed immunostaining of control fly brains with a dPPIL4 antibody. dPPIL4 was broadly expressed in the soma and predominantly localized in the nucleus (Figures 2D and 2E). Co-staining of the core clock protein PER showed that dPPIL4 was expressed in clock neurons including sLN_vs, lLN_vs, LN_ds, and DNs (Figures 2E and 2F). In *dppil4* KD flies, dPPIL4 signals were markedly diminished in clock neurons (Figure S4). Notably, the reduction in dPPIL4 levels was more pronounced in the LN_ds and DN1s compared to the sLN_vs, and lLN_vs, although the differences were not statistically significant (Figure S4). Given that the dPPIL4 levels were consistent across clock neurons in control flies, this variability likely reflects differences in the effectiveness of RNAi-mediated knockdown among clock neurons, potentially contributing to the residual dPPIL4 signals observed in the sLN_vs, and lLN_vs (Figure S4).

In addition, although dPPIL4 protein levels in whole head extracts were constant throughout the day (Figure 2B), they might still be rhythmically expressed in clock neurons. To examine this possibility, we measured dPPIL4 levels in sLN_vs throughout the day (Figure 2G) and found that dPPIL4 was not rhythmically expressed in sLN_vs (Figure 2H).

Reduction of PER levels is responsible for the long period of dPPIL4 KD flies

Within the clock neuron network, sLN_vs play a crucial role in governing free-running rhythms, thereby determining the circadian period.[36–39] To understand the mechanism underlying circadian rhythm defects induced by *dppil4* KD, we examined the molecular rhythms of core clock proteins in sLN_vs under the LD cycle condition (Figures 3A–3H). In *dppil4* KD flies, PER levels were greatly reduced throughout the day, and the oscillation phase was slightly delayed compared to control flies (Figures 3A and 3B). However, the TIM levels in *dppil4* KD flies were comparable to those in control flies (Figures 3C and 3D). Additionally, while TIM protein was mostly located in the nucleus at ZT 22 in control flies, TIM protein was still in the cytoplasm in *dppil4* KD flies, indicating delayed nuclear accumulation of TIM (Figure 3C; Figure S5). Given that PER levels were lower in the *dppil4* KD flies, this is consistent with the previous reports that PER is required for nuclear entry of TIM.[13,40,41] Next, we examined the CLK and VRI levels at their respective peak and trough time points and found no differences between control and *dppil4* KD flies (Figures 3E–3H). Collectively, among the core clock proteins examined, only the PER level was greatly reduced in *dppil4* KD flies. Under DD condition, the PER levels in sLN_vs of *dppil4* KD flies were lower and showed a delayed oscillation phase compared with control flies, which is consistent with the long period of these flies (Figure 3I).

To investigate whether PER level reduction caused the long period of *dppil4* KD flies, we overexpressed the UAS-*per* transgene using TUG in the *dppil4* KD background and analyzed the circadian rhythm behavior. To ensure an equivalent dosage of the UAS transgene, we expressed UAS-*gfp* instead of UAS-*per* in control conditions. Flies expressing UAS-*gfp* or UAS-*per* alone manifested a quasi-normal period with comparable rhythmicity. Downregulation of *dppil4* lengthened the period to 28.9 h. When the UAS-*per* transgene was expressed in *dppil4* KD background, the long periodicity was significantly attenuated to 25.6 h (Figure 3J; Table S4). Taken together, these results indicate that dPPIL4 controls the circadian rhythm speed by affecting the PER level in *Drosophila*.

dPPIL4 regulates both *per* RNA and protein levels

To investigate how dPPIL4 regulates PER levels in flies, we measured pre-mRNA and mRNA levels of *per* during the LD cycle. Both *per* pre-mRNA and mRNA levels were reduced in *dppil4* KD flies compared to control flies, suggesting that dPPIL4 regulates *per* transcription (Figure 4A). Consistent with the lack of effects on other clock protein levels by dPPIL4 KD, *tim* pre-mRNA and mRNA levels showed no difference between the control and *dppil4* KD conditions (Figure 4B). *per* transcription is initiated by binding of CLK and CYC at its promoter. To determine whether dPPIL4 is involved in this process, we expressed the *per7.2:9* transgene, which lacks the 5′ flanking region, first exon (noncoding), and most of the first intron of *per,* in the per^{01} background and monitored the effect of *dppil4* KD.[42,43,44] (Figures 4C and 4D; Table S5). As a control, 13.2-kb genomic *per* was expressed instead of the mutant *per*. Consistent with previous findings, expression of 13.2-kb genomic *per* rescued the arrhythmicity of per^{01} and restored the period to 24.3 h.[45] Downregulation of *dppil4* in this genetic background lengthened the period by 4.6 h. In flies with the *per7.2:9* transgene in the per^{01} background, *per7.2:9* mRNA was rhythmically expressed through post-transcriptional regulation. PER protein exhibited reduced levels and a delayed phase, resulting in a long circadian rhythm period of 26.3 h.[43,44] Downregulation of *dppil4* in the *per7.2:9* transgene-expressing background further lengthened the period by approximately 4.5 h, similar to the effect observed in flies expressing the 13.2-kb genomic *per*. Two-way ANOVA analyses validated that the period lengthening effect of *dppil4* KD and *per7.2:9* transgene expression was additive (Figure 4E). PER levels in sLN_vs were measured during the early night (ZT18), when PER is actively synthesized, and early morning (ZT2), when PER degradation is predominant. In flies expressing the 13.2-kb genomic *per, dppil4* KD greatly reduced PER levels in sLN_vs at both ZT18 and ZT2 (Figures 4G and 4H). Similarly, in flies with the per^{01};*per7.2:9* genetic background, PER levels in sLN_vs were lower under *dppil4* KD. Because promoterless *per7.2:9* transgene-induced *per* expression was affected by *dppil4* KD, we concluded that dPPIL4 does not regulate the CLK/CYC-dependent transcription initiation process.

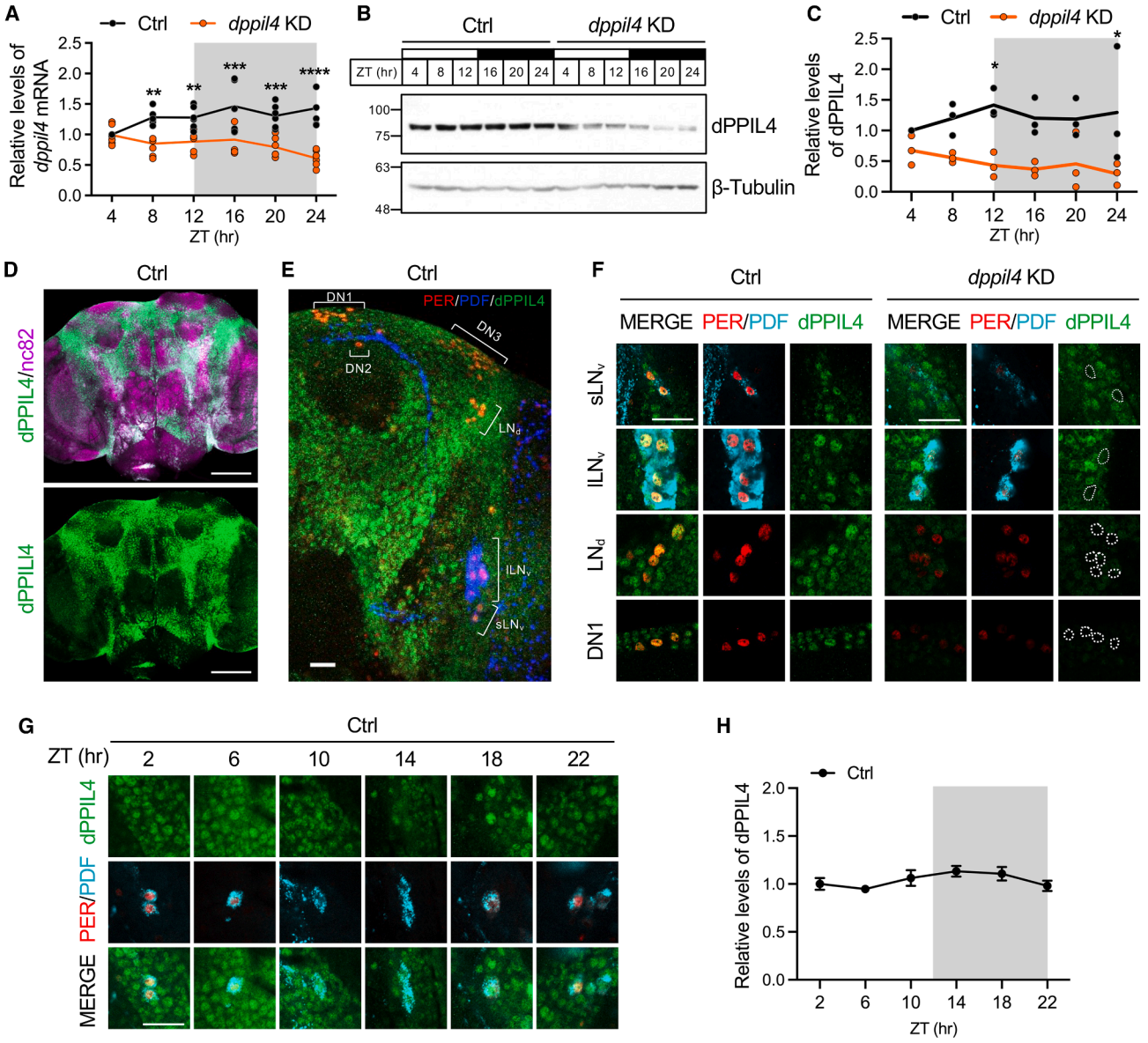

Figure 2. dPPIL4 was broadly expressed in brain cells, including clock neurons, and localized in the nucleus

(A) The *dppil4* mRNA levels were quantified throughout the daily cycle in control (TUG>*d2*) and *dppil4* KD (TUG>*d2, dppil4* Ri*)* flies using real-time qRT-PCR. ZT = zeitgeber time. Statistically significant differences were analyzed using two-way ANOVA followed by Sidak's multiple comparisons test (*$p < 0.05$, **$p < 0.01$, ***$p < 0.001$, ****$p < 0.0001$, $n = 4$).

(B) Protein extracts were prepared from the heads of indicated flies throughout the daily cycle and were analyzed by immunoblotting with an anti-dPPIL4 (Gp2) antibody. β-Tubulin served as the loading control. A representative image from four independent experiments is shown. See Figure S3 for anti-dPPIL4 antibody validation result.

(C) Quantification of dPPIL4 levels, which are normalized to β-Tubulin levels, is shown. Statistically significant differences were analyzed using two-way ANOVA followed by Sidak's multiple comparisons test (*$p < 0.05$, $n = 3$).

(D) Control flies were dissected at ZT2 and stained with anti-dPPIL4 (Gp1, green) and anti-nc82 (magenta) antibodies. Scale bars represent 100 μm.

(E and F) Control and *dppil4* KD flies were dissected at ZT2 and stained with anti-dPPIL4, anti-PER, and anti-PDF antibodies. Scale bars represent 20 μm. (E) dPPIL4 was broadly expressed in the cell bodies in the brain. (F) dPPIL4 was expressed in the nuclei of clock neurons, including sLN_vs, lLN_vs, LN_ds, and DN1s. In addition, dPPIL4 levels were greatly reduced in the clock cells of *dppil4* KD flies (white dotted circles). $n = 13–49$ (G) Control (TUG>*d2*) flies were dissected at the indicated times, and the brains were processed for whole-mount immunohistochemistry with anti-dPPIL4, anti-PER, and anti-PDF antibodies. Scale bars represent 20 μm.

(H) The fluorescence intensities of dPPIL4 in sLN_vs were quantified. Values indicate the mean ± SEM (Brain = 8-10 and $n = 25–38$). Metacycle analysis was conducted to assess the rhythm of dPPIL4 (BH q = 0.380).

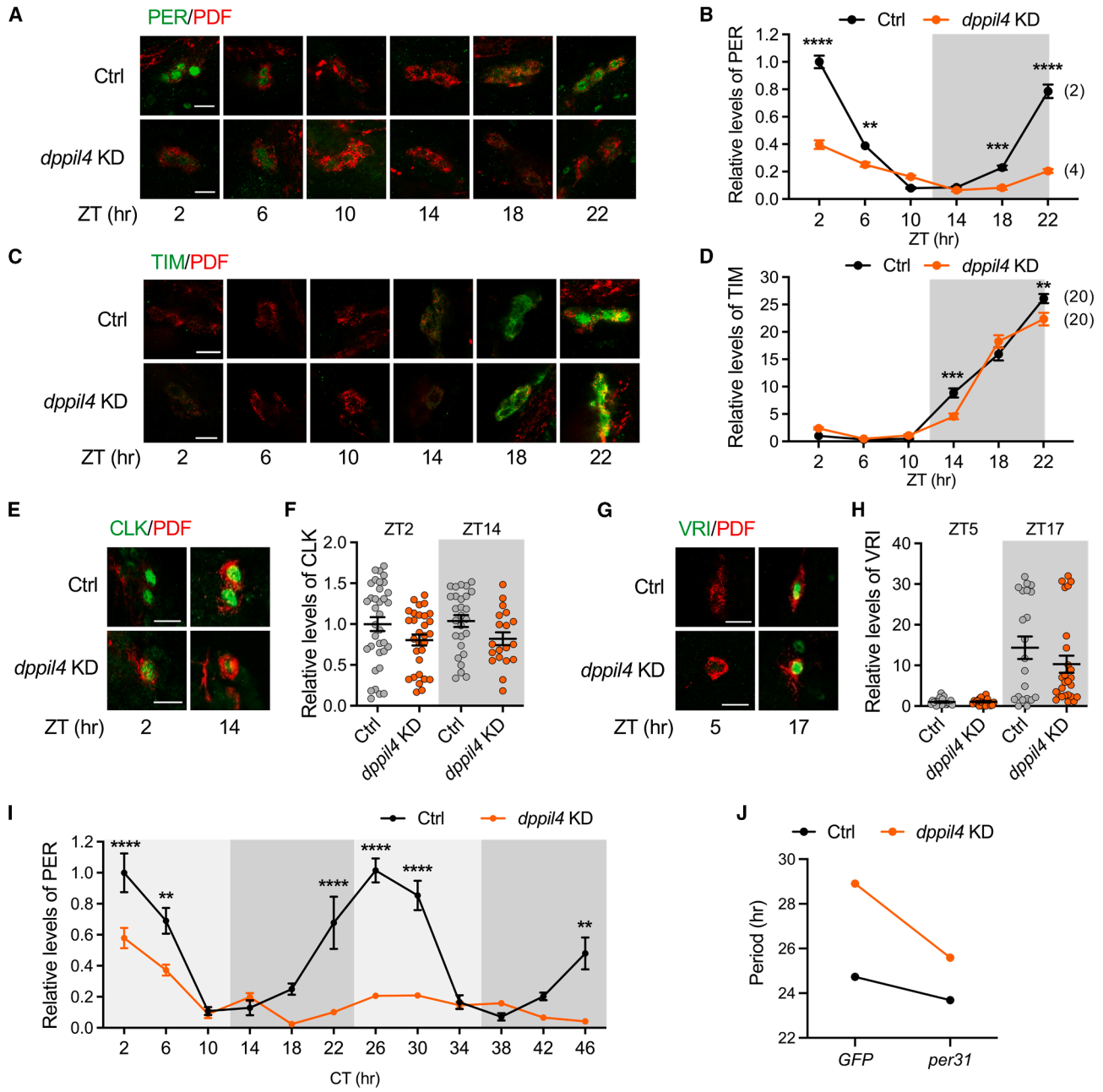

Figure 3. PER levels were reduced in *dppil4* KD flies and *per* expression restored the long period of *dppil4* KD flies

(A–D) Control (TUG>*d2*) and *dppil4* KD (TUG>*d2, dppil4* Ri) flies were dissected at the indicated times, and the brains were processed for whole-mount immunohistochemistry with anti-PER or anti-TIM and PDF antibodies. The fluorescence intensities of sLN_vs are shown. Scale bars represent 10 μm. (B) PER fluorescence intensities were quantified. Values indicate the mean ± SEM. Statistically significant differences were analyzed using two-way ANOVA followed by Sidak's multiple comparisons test (**$p < 0.01$, ***$p < 0.001$, ****$p < 0.0001$, n = 23–38). The phase, determined using Metacycle analysis, is indicated in parentheses (BH q < 0.0001). Notably, the phase in *dppil4* KD flies is significantly delayed compared to control flies. (D) TIM fluorescence intensities were quantified. Values indicate the mean ± SEM. Statistically significant differences were analyzed using two-way ANOVA followed by Sidak's multiple comparisons test (**$p < 0.01$, ***$p < 0.001$, n = 16–20). The phase, determined using Metacycle analysis, is indicated in parentheses (BH q < 0.0001).

(E–H) Control (TUG>*d2*) and *dppil4* KD (TUG>*d2, dppil4* Ri) flies were dissected at the indicated times, and the brains were processed for whole-mount immunohistochemistry with anti-CLK or anti-VRI and anti-PDF antibodies. Fluorescent images of sLN_vs are shown. (F) CLK fluorescence intensities were quantified. Values indicate the mean ± SEM. Statistically significant differences were analyzed using Mann-Whitney test (n = 19–35). (H) VRI fluorescence intensities were quantified. Values indicate the mean ± SEM. Statistically significant differences were analyzed using Mann-Whitney test (n = 19–35). Please note that there were no significant differences in CLK or VRI levels between control and *dppil4* KD flies.

(legend continued on next page)

Next, we analyzed whether dPPIL4 is involved in the post-translational regulation of PER using flies in which *per* was expressed by the UAS-*per31* cDNA construct under the control of TUG. TUG-driven expression of *per* cDNA rescued the arrhythmicity of per^{01} flies and restored the period to 23.9 h. Knockdown of *dppil4* in these flies lengthened the period to 26.9 h (Figure 4D; Table S5). Interestingly, the extent of period lengthening due to *dppil4* KD in UAS-*per31*-expressing flies was less pronounced than in other lines. Two-way ANOVA analysis confirmed that the period lengthening effect of dppil4 KD was significantly reduced in the UAS-*per*31-expressing flies (Figure 4F). PER levels under *dppil4* KD in UAS-*per*31 expressing flies were comparable to control flies at ZT18 and even higher at ZT2 (Figures 4G and 4H). These results suggest that *per* transcription driven by the *per* cDNA construct is less affected by *dppil4* KD, and the regulatory role of dPPIL4 likely depends on the genomic structure of *per* including both exons and introns. This dependency might explain why the PER level at ZT18 was not reduced by knocking down *dppil4*. Moreover, dPPIL4 appears to destabilize the PER protein in the early morning when PER is actively degraded in the nucleus. To confirm that the increased PER levels were not simply a result of delayed degradation due to the lengthened circadian period, we compared the PER levels in control and *dppil4* KD flies at the same internal time, accounting for their circadian period differences (Figure S6). PER levels in *dppil4* KD flies expressing *per* cDNA were higher than in control flies, indicating that dPPIL4 enhances the degradation of PER protein. Collectively, we concluded that dPPIL4 regulates PER abundance at both the RNA and protein levels.

dPPIL4 supports *per* transcription by augmenting RNAPII CTD phosphorylation

Several studies have indicated that dPPIL4 orthologs regulate RNAPII activity in *C.elegans, A.thaliana,* and *S.pombe.*[47–50] Since *dppil4* KD reduced *per* mRNA levels without affecting CLK/CYC-dependent transcription initiation (Figures 4C and 4D), we hypothesized that dPPIL4 enhances *per* transcription by influencing RNAPII activity. RNAPII, a multi-subunit complex, includes the core subunit Rpb1 encoded by *Polr2A* and smaller subunits Rpb5, Rpb6, Rpb8 encoded by *Polr2E*, *Polr2F*, and *Polr2H* respectively.[51,52] Activation of RNAPII involves phosphorylation of the Rpb1 C-terminal domain (CTD) heptapeptide repeats at Ser5 and Ser2 residues.[53,54] Ser5 phosphorylation facilitates the transition from initiation to early elongation, 5′-capping while Ser2 phosphorylation promotes elongation and the maturation process.[55–57]

To investigate whether RNAPII activity is affected by dPPIL4, we measured Ser5 (pSer5) and Ser2 (pSer2) phosphorylation on the RNAPII CTD in control and *dppil4* KD flies at ZT12 and ZT24. In control flies, although the total RNAPII CTD pSer2 level was similar at ZT12 and ZT24, the pSer5 level was higher at ZT12 than at ZT24, indicating that early elongation of transcription was more active at ZT12 than at ZT24 (Figures 5A and 5B). Importantly, RNAPII CTD pSer5 level in *dppil4* KD flies was reduced compared to control flies at ZT12. Given that *per* transcription actively occurs during the mid-day, this result correlates with the reduction of *per* pre-mRNA levels in *dppil4* KD flies (Figure 4A). CTD pSer2 and total RNAPII levels were not affected by *dppil4* downregulation. To confirm whether dPPIL4 interacts with RNAPII, we performed an immunoprecipitation (IP) assay. dPPIL4 antiserum specifically pulled down RNAPII protein at both ZT12 and ZT24. These results suggest that dPPIL4 supports *per* transcription by augmenting RNAPII CTD Ser5 phosphorylation.

To test whether RNAPII subunit knockdown replicates the circadian phenotypes observed in *dppil4* KD flies, we performed RNAi-mediated knockdowns of *Polr2A*, *Polr2E*, *Polr2F*, and *Polr2H* using the TUG driver (Table S6; Figures 5D and 5E). RT-PCR confirmed efficient knockdown (Figure S7). *Polr2A* (encoding core subunit Rpb1) KD rendered flies arrythmic, while *Polr2E* or *Polr2F* (encoding Rpb5 and Rpb6, respectively) KD lengthened the circadian period by approximately 1h. *Polr2H* (encoding Rpb8) KD had no effect. The stronger phenotype observed in *Polr2A* KD flies compared to *dppil4* KD flies may result from a global dysfunction of RNAPII from reduction in Rpb1 levels, as compared to modulation of RNAPII activity via CTD phosphorylation. Notably, the period lengthening observed in *Polr2E* or *Polr2F* KD flies, which modulate RNAPII activity,[58–60] aligns with the long period phenotype of *dppil4* KD flies although the effect was smaller.

Because RNAPII CTD pSer5 levels were reduced by dPPIL4 KD, it might affect transcription more globally. To assess this, we performed RNA-Seq analysis on RNA extracted from fly heads at ZT8 and ZT16 (Figure 5F). The analysis revealed that dPPIL4 KD significantly influenced gene expression. 60 genes downregulated and 215 genes upregulated up at ZT8 (BH $p < 0.05$) and 172 genes downregulated and 128 genes upregulated up at ZT16 (BH $p < 0.05$) (Supplemental file 1). Importantly, among clock genes, *per* mRNA levels were consistently and significantly reduced at both time points. In contrast, *tim* and *vri* mRNA levels were selectively reduced at ZT8 and ZT16, respectively, while the expression of other clock genes (*Clk*, *cyc*, *pdp1*) remained unaffected. We propose that the reductions in *tim* and *vri* mRNA levels were insufficient to significantly impact TIM and VRI protein levels. However, the persistent reduction in *per* mRNA correlated with the pronounced decrease in PER protein levels. These results underscore a more pronounced transcriptional defect in *per* regulation caused by dPPIL4 KD.

(I) Control (TUG>*d2*) and *dppil4* KD (TUG>*d2, dppil4* Ri) flies were dissected at the indicated times after 2 days of the DD condition. The fluorescence intensities of PER in sLN_vs are shown. The PER oscillation amplitude was greatly reduced, and the phase was delayed in *dppil4* KD flies compared with those in control flies. Values indicate the mean ± SEM. Statistically significant differences were analyzed using two-way ANOVA followed by Sidak's multiple comparisons test (**$p < 0.01$, ****$p < 0.0001$, $n = 10–27$).

(J) Graph represents the period lengths in Ctrl (TUG>*d2*) and *dppil4* KD (TUG>*d2, dppil4* Ri) flies with UAS-*GFP* or UAS-*per31* expression. Values indicate mean ± SEM. two-way ANOVA showed significant effects of *dppil4* knockdown ($F_{(1,182)} = 858.6$, $p < 0.0001$), *per* overexpression ($F_{(1,182)} = 441.5$, $p < 0.0001$), and their interaction ($F_{(1,182)} = 120.7$, $p < 0.0001$). $n = 16–72$.

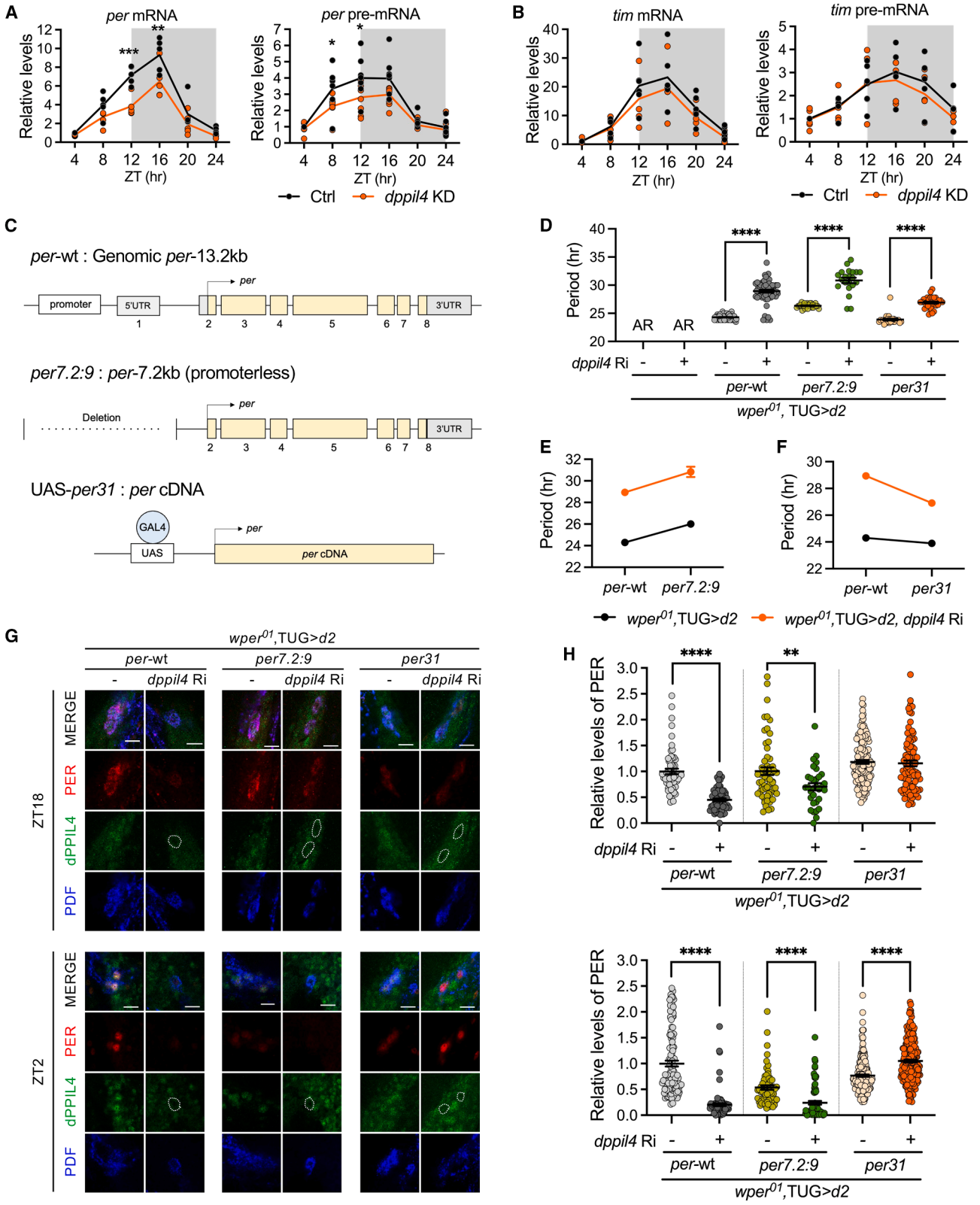

(legend on next page)

Given that RNAPII CTD interacts with the spliceosome to facilitate gene expression,[55] and that orthologs of dPPIL4 are known to interact with splicing factor,[47,50,61,62] we investigated whether dPPIL4 specifically affects *per* transcription among core clock genes through splicing. However, DEXseq analysis revealed no statistically significant changes in *per* exon junctions in *dppil4* KD flies compared to controls (Figures 5G and 5H). These findings suggest that dPPIL4-dependent regulation of *per* transcription is unlikely to involve splicing mechanisms.

In conclusion, our results demonstrate that dPPIL4 supports per transcription by enhancing RNAPII CTD Ser5 phosphorylation, particularly during periods of active transcription.

dPPIL4 stabilizes Cullin1 to promote PER degradation

While *dppil4* KD did not upregulate PER levels expressed from the genomic construct, PER levels expressed from UAS-*per31* transgene were increased in the sLN_vs of *dppil4* KD flies compared to controls at ZT2 (Figures 4G and 4H). This suggests that dPPIL4 facilitates PER degradation during the early morning after PER translocates to the nucleus. The lack of increased PER levels in the genomic *per* context under *dppil4* KD may be due to inherently low PER levels from reduced mRNA expression, limiting the substrate available for degradation. To directly assess whether dPPIL4 regulates PER degradation during the early morning. we compared the PER degradation rate between control and *dppil4* KD flies following CHX treatment. After 3 h of fasting, flies were fed either vehicle (EtOH) or 5 mM CHX in high-sucrose food starting from ZT0. Both control and *dppil4* KD flies ingested comparable amounts of CHX-containing food (Figure 6A). PER levels in sLN_vs were quantified every hour following treatment. In CHX-treated control flies, PER degradation was accelerated compared to EtOH-treated control, confirming effective inhibition of PER translation by CHX (Figures 6B and 6C). However, CHX-treated *dppil4* KD flies exhibited much slower PER degradation than controls, indicating that dPPIL4 facilitates PER degradation in the early morning when PER is in the nucleus.

To investigate whether dPPIL4 physically interacts with PER to influence its degradation, we performed reciprocal IP assays at ZT22, 0, and 2 when PER is predominantly nuclear. These assays revealed no physical interaction between PER and dPPIL4 (Figure S8). This suggests that dPPIL4 regulates PER degradation indirectly.

Hyper-phosphorylated PER is targeted for degradation by the 26S proteasome after ubiquitination by the SCF ubiquitin ligase complex.[15–17] In *dppil4* KD flies, the levels of CUL1, a core SCF component, were reduced compared to controls (Figures 6D and 6E). The specificity of CUL1 antiserum was validated in CUL1-overexpressing and KD flies (Figure S9). Furthermore, IP assays in control flies demonstrated a physical interaction between CUL1 and dPPIL4 (Figure 6F). These results indicate that dPPIL4 stabilizes CUL1, thereby maintaining the SCF complex's activity to facilitate PER degradation. Given that reduction in CUL1 could broadly impair SCF complex activity in dPPIL4 KD flies, we analyzed the levels of Cubitus interruptus (Ci), another SCF complex substrate.[63,64] Ci levels were elevated in dPPIL4 KD flies, compared to controls (Figure S10). These findings highlight the essential role of dPPIL4 in maintaining SCF complex stability and function, ensuring the proper degradation of multiple substrates, including PER and Ci.

In conclusion, we propose a model where dPPIL4 regulates the circadian rhythm by dual mechanisms. In the clock cell nucleus, dPPIL4 supports *per* transcription by augmenting RNAPII activity during mid-day. dPPIL4 also secures the SCF complex by increasing the CUL1 level, resulting in efficient degradation of PER in the early morning. These processes collectively produce high-amplitude PER oscillations, essential for robust 24-h rhythmicity (Figure 6G).

DISCUSSION

In this study, we identified that dPPIL4, a member of the cyclophilin family, plays a crucial role in regulating the circadian rhythm in *Drosophila*. KD of *dppil4* significantly dampened the amplitude of the PER molecular rhythm in core clock neurons,

Figure 4. dPPIL4 regulated both *per* RNA and protein levels

(A and B) Control and *dppil4* KD flies were entrained under a 12L:12D cycle. Flies were collected at the indicated times and processed for real-time qRT-PCR to measure pre-mRNA and mRNA levels of *per* (A) and *tim* (B). Values represent the mean ± SEM. (A) For *per* mRNA, statistically significant differences were analyzed using two-way ANOVA followed by Sidak's multiple comparisons test (**$p < 0.01$, ***$p < 0.001$, $n = 5$). For *per* pre-mRNA, statistically significant differences were analyzed using two-way ANOVA followed by Sidak's multiple comparisons test (*$p < 0.05$, $n = 8$). (B) For *tim* mRNA, statistically significant differences were analyzed using two-way ANOVA followed by Sidak's multiple comparisons test ($n = 5$). For *tim* pre-mRNA, statistically significant differences were analyzed using two-way ANOVA followed by Sidak's multiple comparisons test ($n = 5$).

(C) Schematic diagram of *period* transgenes. *per*-wt indicates the genomic *per* transgene, which has a 13.2-kb wild-type *per* locus. *per7.2:9* is a promoterless transgene, and *per* is expressed by an enhancer-trapped gene promoter[42,43] UAS-*per31* consists of *per* cDNA downstream of UAS, which is thereby expressed by GAL4.[46] (D–F) *per*-wt, *per*7.2:9, or UAS-*per*31 was expressed in the per^{01} background in combination with control (−) or *dppil4* Ri (+). (D–F) The free-running periods of flies are shown, with genotypes indicated below. Values indicate the mean ± SEM. AR = arrhythmic. Statistically significant differences were analyzed using one-way ANOVA followed by Sidak's multiple comparisons test (****$p < 0.0001$, $n = 21–77$). See Table S5 for additional details of behavior analysis. (E and F) two-way ANOVA analyses of the free-running periods shown in D revealed significant effects of *dppil4* knockdown ($F_{(1,180)} = 415.7$, $p < 0.0001$), and *per* transgene expression ($F_{(1,180)} = 59.74$, $p < 0.0001$), but no significant interaction ($F_{(1,180)} = 0.1673$, $p = 0.6830$). $n = 21–77$. (E) Significant effects of *dppil4* knockdown ($F_{(1,191)} = 390.9$, $p < 0.0001$), *per* transgene expression ($F_{(1,191)} = 39.67$, $p < 0.0001$), and their interaction ($F_{(1,191)} = 17.48$, $p < 0.0001$). $n = 26–77$. (F).

(G and H) Flies were dissected at the indicated times, and isolated brains were processed for whole-mount immunohistochemistry. Brains were co-stained with anti-dPPIL4, anti-PER, and anti-PDF antibodies. Fluorescent images of sLN_vs are shown. The white dotted circles indicate sLN_vs of dPPIL4 KD flies. The scale bar represents 10 μm. (H) PER fluorescence intensities were quantified. Values indicate the mean ± SEM. For ZT18, Statistically significant differences were analyzed using one-way ANOVA followed by Sidak's multiple comparisons test (**$p < 0.01$, ****$p < 0.0001$, $n = 32–143$). For ZT2, Statistically significant differences were analyzed using one-way ANOVA followed by Sidak's multiple comparisons test (****$p < 0.0001$, $n = 32–143$). See Figure S6 for comparison of PER levels at the same internal CT.

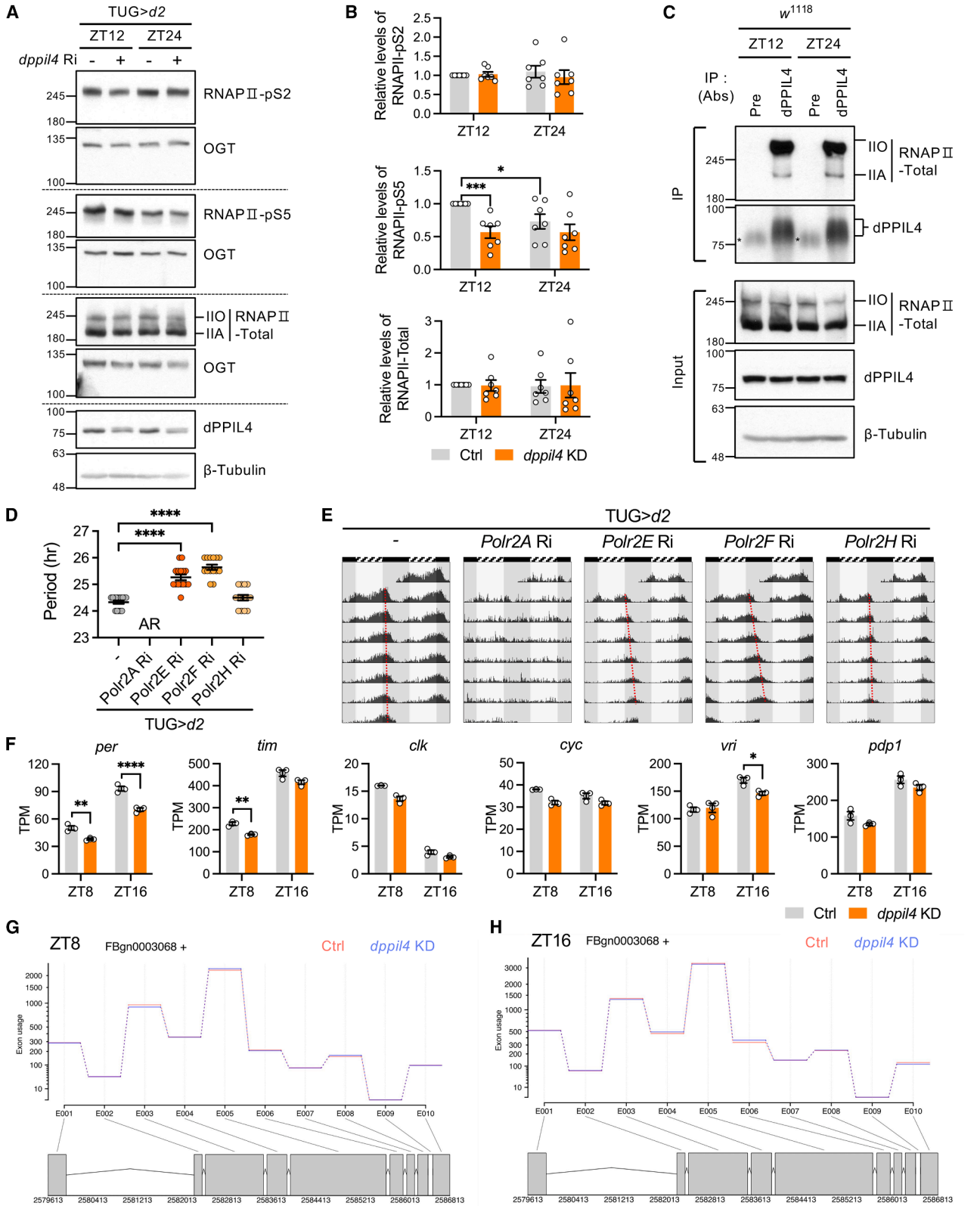

(legend on next page)

resulting in a long circadian period. We further revealed that KD of *dppil4* was associated with attenuated RNAPII CTD Ser5 phosphorylation and reduced levels of CUL1 in the SCF complex. These findings suggest a unique regulatory role for dPPIL4 in regulating PER abundance by influencing both its synthesis during the early phase and its degradation during the later phase of the circadian cycle. We propose that this dual regulatory role of dPPIL4 ensures precise control over PER levels, thereby supporting a robust circadian rhythm.

KD of *dppil4* reduced both *per* pre-mRNA and mRNA levels, indicating that *per* transcription is influenced by dPPIL4 (Figure 4A). Regarding the mechanism through which dPPIL4 supports *per* transcription, we initially hypothesized that dPPIL4 might regulate the activity of the circadian transcription factors CLK/CYC because several PPIases interact with transcription factors and modulate the expression of downstream target genes.[24] However, this possibility was excluded because *per* expression driven by promoterless *per7.2:9* transgene, which bypasses CLK/CYC mediated initiation, was also affected by *dppil4* KD (Figures 4D and 4H). We then proposed that dPPIL4 modulates RNAPII activity to regulate *per* transcription, based on the following evidence. First, dPPIL4 orthologs in other organisms, such as SIG-7 *in Caenorhabditis elegans* and Rct1 in *Saccharomyces pombe,* enhance RNAPII activity by increasing pSer2 and pSer5 level,[48,50] while AtCyp59 in *Arabidopsis* reduces RNAPII pSer5 levels and overall activity.[47] These studies underscore the conserved role of dPPIL4 orthologs in regulating RNAPII. Similarly, our data show that dPPIL4 influences RNAPII pSer5 levels in *Drosophila* (Figures 5A and 5B). Second, dPPIL4 physically interacts with RNAPII (Figure 5C), further supporting its role in RNAPII regulation. Third, the mammalian ortholog PPIL4 interacts with Jumonji domain-containing 6 (JMJD6), a key regulator of RNAPII pause-release at promoter,[65] and increase JMJD6 levels, linking PPIL4 to transcriptional regulation.[66] Additionally, functional analysis of RNAPII subunits further supports the role of dPPIL4 in RNAPII activity. Knockdown of the core RNAPII subunit Rpb1 caused severe behavioral defects, making flies arrhythmic, likely due to a global dysfunction of RNAPII. KD of Rpb5 and Rpb6, which plays a modulatory role of RNAPII activity, resulted in a lengthened circadian period, resembling the phenotype of dPPIL4 KD (Figures 5D and 5E). Collectively, our findings suggest that dPPIL4 supports *per* transcription by modulating RNAPII activity. Nonetheless, the observed reduction in RNAPII pSer5 levels and *per* mRNA levels remains correlative, more definitive studies are warranted to clarify the causal relationship between RNAPII pSer5 levels and *per* mRNA/PER protein abundance.

Although dPPIL4 influenced *per* RNA transcription it did not consistently affect the mRNA levels of other core clock genes (Figures 4B and 5F). We initially hypothesized that splicing factors might mediate the *per*-specific transcriptional regulation by dPPIL4, given that the effect of dPPIL4 KD on PER levels depended on a genome structure including exons and introns and was minimal when PER was expressed from *per* cDNA (Figures 4D and 4F). Supporting this idea, several PPIases are known to associate with splicing factors[24,67] including PPIL4, which is a component of the human spliceosome[68,69] and dPPIL4 orthologs in *Arabidopsis thaliana*[47] and *Caenorhabditis elegans*[50] which regulate co-transcriptional splicing. However, our splicing analysis of the *per* gene showed no significant splicing differences in *dppil4* KD compared to controls (Figures 5G and 5H), suggesting that our initial hypothesis may not hold. Interestingly, phosphorylation of the RNAPII CTD has been shown to influence multiple transcriptional stages, with its role varying significantly among genes. For instance, inhibiting CTD Ser-5 phosphorylation kinase results in gene-specific downregulation rather than a uniform effect.[70,71] Furthermore, genome-wide mapping of CTD phosphorylation dynamics in *Saccharomyces cerevisiae* revealed variability among genes based on promoter structure and expression levels.[72] Notably, gene-specific effects of CTD phosphorylation have been observed not only for Ser5 but also for Ser2, further highlighting the complexity of its regulation.[73] Collectively, these results suggest that the effect of RNAPII CTD Ser5 phosphorylation might vary in a gene-specific manner, with *per* being particularly sensitive to such regulation.

How might dPPIL4 regulate RNAPII CTD phosphorylation? Given that dPPIL4 interacts with RNAPII (Figure 5C) and functions as a PPIase, we propose that dPPIL4 could induce conformational changes in RNAPII through isomerization, thereby

Figure 5. dPPIL4 interacted with and regulated RNAPII CTD phosphorylation

(A) Control (−) and *dppil4* KD (+) flies were collected at ZT12 and ZT24, and head protein extracts were analyzed by western blotting with anti-RNAPII-pSer2, anti-RNAPII-pSer5, anti-RNAPII-total, and anti-dPPIL4 antibodies. O-GlcNAc transferase (OGT) and β-Tubulin served as loading controls. Representative images of seven independent experiments are shown.

(B) Relative levels of RNAPII-pSer2, RNAPII-pSer5, and RNAPII-total are quantified. Values represent the mean ± SEM. Statistically significant differences were analyzed using Student's *t* test or Mann-Whitney test. (*$p < 0.05$, ***$p < 0.001$, $n = 7$).

(C) w^{1118} flies were collected at ZT12 and ZT24. Head protein extracts were processed for immunoprecipitation with an anti-dPPIL4 antibody (Gp1). Asterisks indicate non-specific band of dPPIL4. Immune complexes were analyzed by immunoblotting with an anti-RNAPII-total and an anti-dPPIL4 antibody. Hyper-phosphorylated isoforms = IIO, hypo-phosphorylated isoforms = IIA.

(D) RNAPII subunit RNAi lines were crossed with TUG>*d2* flies, and their locomotor activity rhythms were analyzed. The free-running periods are shown. Values indicate the mean ± SEM. Statistically significant differences between control and KD flies were analyzed by one-way ANOVA followed by Dunnett's multiple comparisons test (****$p < 0.0001$, $n = 14$–15). See Table S6 for additional details of behavior analysis.

(E) Actograms of flies during seven consecutive days of the DD condition after 4 days of LD entrainment. Actograms are double-plotted to better visualize the rhythmic behavior. Hatched horizontal bars represent subjective day, and black horizontal bars represent subjective night. The dotted red lines connect the evening peaks for each day of the experiment. $n = 13$–16.

(F) Expression levels of core clock genes were quantified using RNA-seq, represented as Transcripts Per Million (TPM). Values represent the mean ± SEM (**BH $p < 0.01$, *** BH $p < 0.001$, and *** BH $p < 0.0001$). $n = 3$.

(G and H) Exon usage of per (FBgn0003068) at ZT8 (G) and ZT16 (H) was analyzed using RNA-seq data processed through DEXSeq. $n = 3$.

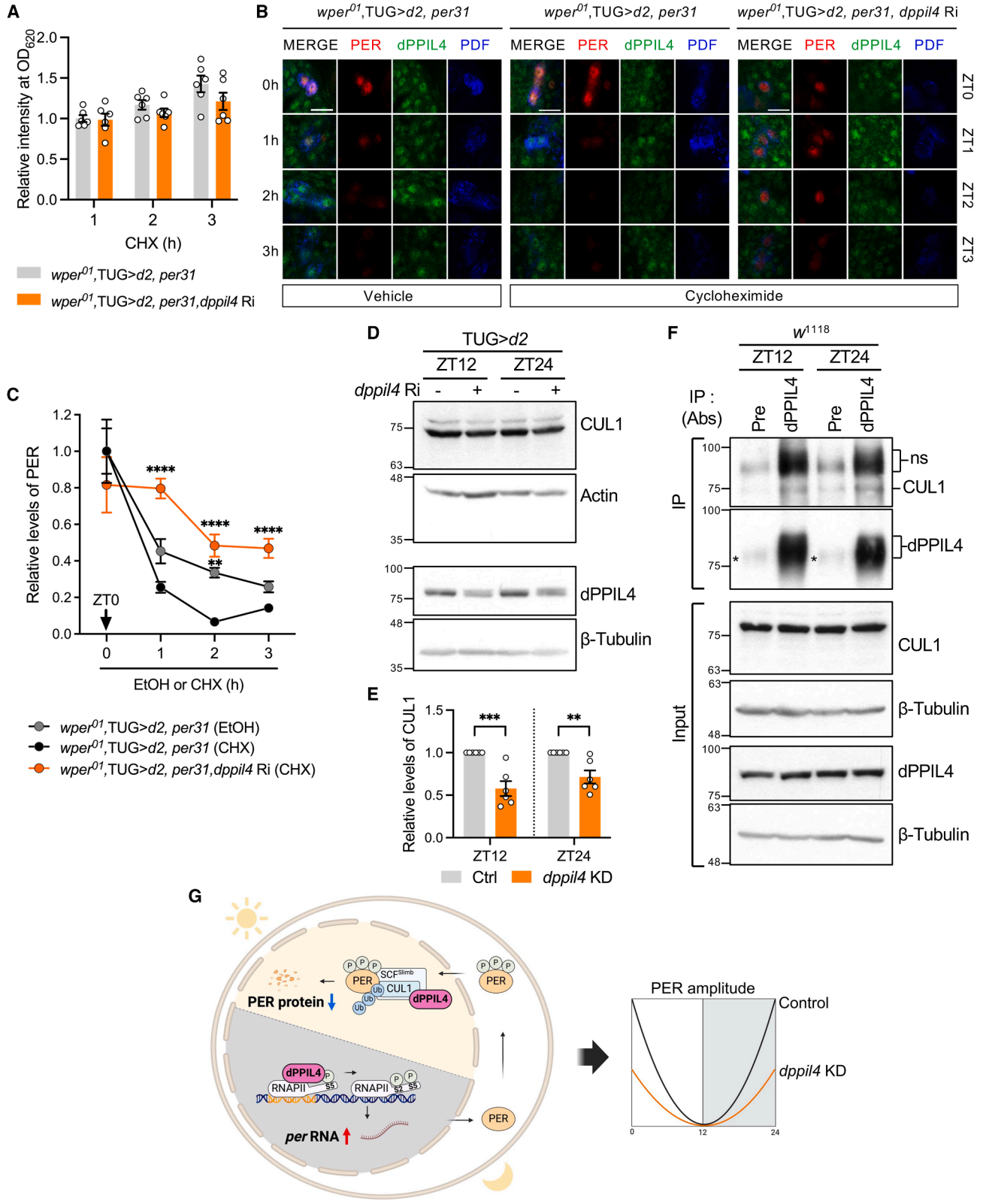

(legend on next page)

modulating its accessibility to enzymatic activity. For instance, RNAPII Ser5 is primarily phosphorylated by CDK7 in the TFIIH complex[54,74,75] and dephosphorylated by the phosphatase Ssu7.[76] Conformational changes mediated by dPPIL4 might enhance RNAPII's interaction with kinases like CDK7 or reduce its interaction with phosphatases like Ssu72 leading to an increase in RNAPII-pS5 levels. Alternatively, dPPIL4 might indirectly influence RNAPII by modulating the activity or stability of CDK7 and/or Ssu72, Further studies are necessary to identify specific substrate affected by the conformational changes induced by dPPIL4.

Given the reduction in PER levels in *dppil4* KD flies, it is plausible that this could indirectly affect the expression of other clock genes such as *Clk* and *vri* through the interlocked feedback loop. In per^{01} flies, CLK levels are reported to be low, while VRI levels are high or intermediate.[6,77] However, in dPPIL4 KD flies under LD conditions, the levels of CLK and VRI were comparable to those in control flies. It might be because the reduction in PER levels in dPPIL4 KD flies may not have been substantial enough to alter the transcription of other core clock components. Despite this, a delay in TIM nuclear accumulation was observed in dPPIL4 KD flies, similar to the phenotype reported in per^{01} flies. The delayed nuclear accumulation of TIM may depend on a stochiometric interaction with PER, highlighting the functional dependency of TIM nuclear accumulation on sufficient TIM levels.

When *per* was expressed using UAS-*per31*, *dppil4* KD increased the PER level at ZT2 (Figures 4G and 4H), suggesting dPPIL4's involvement in the ubiquitination proteasome system (UPS)-mediated PER degradation. As a result, we revealed that dPPIL4 interacted with and stabilized CUL1 (Figures 6D–6F). CUL1, a key scaffold protein in the SCF E3 ligase comple,[78,79] is essential for its activity.[80,81] Reduction of CUL1 by *dppil4* KD would limit the functional SCF complex and thereby slow the PER degradation process as observed in TUG-driven UAS-*per31* flies. Supporting this idea, another substrate degraded by SCF complex, Ci was also increased in *dppil4* KD flies (Figure S10). Nonetheless, when *per* was expressed using the genomic *per* gene, *dppil4* KD did not increase PER levels. We reasoned that although functional SCF E3 ligase complex was reduced, the lower amount of PER from decreased *per* mRNA could be fully degraded by the reduced SCF E3 ligase complex (Figures 3A and 4G). In addition to PER, another core clock protein, TIM, is polyubiquitinated by the SCF^{JETLAG} E3 ligase complex and targeted for degradation by the UPS.[82] Because CUL1 can function as a scaffolding protein of the SCF^{JETLAG} E3 complex as well, TIM protein levels could have been affected by *dppil4* KD, but this was not the case (Figures 3C and 3D). Intriguingly, TIM is also targeted by a CUL3-based ubiquitin ligase complex different from that associated with PER.[83] Moreover, the same study demonstrated that CUL3 could affect TIM degradation in the cytoplasmic compartment in the absence of PER, similar to the effect of *dppil4* KD (Figures 3A and 3C). Thus, we reasoned that a CUL3-based UPS degrades TIM. Therefore, the limited amount of CUL1 produced by *dppil4* KD had a minimal effect on TIM degradation.

In summary, our study demonstrates that PPIase is involved in circadian clock regulation. dPPIL4 regulates both *per* RNA and protein in a time-dependent manner, thereby supporting high-amplitude PER oscillations. To the best of our knowledge, dPPIL4 is the first component found to regulate clock components at both the RNA and protein levels in a time-dependent manner. The preservation of high-amplitude oscillations in clock proteins is pivotal for the robustness of the circadian clock. Conversely, the dampening of the circadian rhythm amplitude is closely associated with aging and various disease conditions. In conclusion, our study not only enhances the understanding of the molecular mechanisms underlying high-amplitude oscillations of clock proteins but also provides new possibilities to explore therapeutic interventions targeting dysfunctional circadian systems.

Limitations of the study

Although we observed alterations in RNA Pol II CTD phosphorylation and CUL1 levels following *dppil4* KD, the isomerization of RNA Pol II and CUL1 by dPPIL4 was not confirmed. Therefore,

Figure 6. dPPIL4 regulated PER protein by stabilizing CUL1 in the SCF complex

(A) The amount of food intake in flies were analyzed. UAS-*per31* was expressed in the per^{01} background singly or in combination with *dppil4* KD. Values represent the mean ± SEM. Statistically significant differences were analyzed using Student's *t* test ($n = 6$). There are no significant differences between the genotypes.

(B and C) UAS-*per31* was expressed in the per^{01} background singly or in combination with *dppil4* KD. Flies were exposed to vehicle (EtOH) or CHX-containing food after 3 h of fasting, collected at the indicated times, and processed for whole-mount immunohistochemistry. Brains were co-stained with anti-dPPIL4, anti-PER, and anti-PDF antibodies. Fluorescence images of sLN_vs are shown. The white dotted circles indicate sLN_vs of dPPIL4 KD flies. The scale bar represents 10 μm. (C) The PER levels were quantified. Statistically significant differences were analyzed using two-way ANOVA followed by Tukey's multiple comparisons test (**$p < 0.01$, ****$p < 0.0001$, $n = 11–56$).

(D) Control (−) and *dppil4* KD (+) flies were collected at ZT12 and ZT24, and head protein extracts were analyzed by western blotting with anti-CUL1 and anti-dPPIL4 antibodies. Actin and β-Tubulin served as loading controls. Representative images of six independent experiments are shown. See Figure S9 for anti-CUL1 antibody validation result.

(E) Relative levels of CUL1 were quantified. Values represent the mean ± SEM. Statistically significant differences were analyzed using Student's *t* test (**$p < 0.01$, ***$p < 0.001$, $n = 6$).

(F) w^{1118} flies were collected at ZT12 and ZT24. Head protein extracts were processed for immunoprecipitation with an anti-dPPIL4 (Gp1) antibody. Asterisks indicate non-specific band of dPPIL4. Immune complexes were analyzed by immunoblotting with an anti-CUL1 and an anti-dPPIL4 antibody.

(G) A schematic diagram of our model shows how dPPIL4 regulates the PER molecular rhythmic amplitude in clock cells. During the mid-day, when *per* is actively transcribed, dPPIL4 regulates the RNAPII pSer5 level, thereby increasing the *per* mRNA level. Later in the morning, when hyper-phosphorylated PER is degraded, dPPIL4 enhances the degradation of PER by supporting the Slimb-containing SCF complex via stabilizing the CUL1 level. As a result, dPPIL4 plays a crucial role in controlling the circadian rhythm by augmenting the PER molecular amplitude in *Drosophila*. This figure was created with BioRender.com (license to S.W.K).

establishing a direct link between dPPIL4, RNA Pol II/CUL1, and circadian rhythm regulation requires further investigation.

RESOURCE AVAILABILITY

Lead contact

Further information and requests for resources and reagents may be directed to and will be fulfilled by the Lead Contact, Dr. Eun Young Kim (ekim@ajou.ac.kr).

Materials availability

Fly strains and antibodies generated in this study are available from the lead contact upon request.

Data and code availability

- RNA sequencing data have been deposited at NCBI and are publicly available as of the data of publication. Accession numbers are listed in the key resources table.
- This paper does not report original code.
- Any additional information required regarding data is available from the lead contact upon request.

ACKNOWLEDGMENTS

This research was supported by National Research Foundation of Korea (NRF) grants funded by the Korean government (Ministry of Science and ICT; grant numbers 2017R1A2B2010334, 2019R1A5A2026045, and RS-2023-00208490). Drosophila stocks obtained from the Bloomington Drosophila Stock Center (NIH P40OD018537) and Vienna Drosophila Resource Center (VDRC, www.vdrc.at) were used in this study. We are very grateful to Paul E. Hardin for providing *per*^{01}*;;per7.2:9* flies and anti-VRI antibodies.

AUTHOR CONTRIBUTIONS

E.Y.K. designed research; S.W.K., H.T.T., G.L., and J.T.L. performed research; S.W.K., H.T.T., S.B.L., and E.Y.K. analyzed data; and S.W.K. and E.Y.K. wrote the paper.

DECLARATION OF INTERESTS

The authors declare no competing interest.

STAR★METHODS

Detailed methods are provided in the online version of this paper and include the following:

- KEY RESOURCES TABLE
- EXPERIMENTAL MODEL AND STUDY PARTICIPANT DETAILS
  - Fly stocks
  - Transgenic fly generation
- METHOD DETAILS
  - Locomotor behavior analysis
  - Western blotting and immunoprecipitation
  - Immunohistochemistry and confocal imaging
  - Real-time quantitative reverse transcription-PCR (qRT-PCR)
  - PER degradation rate analysis: Cycloheximide (CHX) treatment
  - Feeding assay
  - RNA-Sequencing and data analysis
  - DEXseq
- QUANTIFICATION AND STATISTICAL ANALYSIS

SUPPLEMENTAL INFORMATION

Supplemental information can be found online at https://doi.org/10.1016/j.isci.2025.112457.

Received: August 7, 2024
Revised: January 3, 2025
Accepted: April 11, 2025
Published: April 16, 2025

REFERENCES

1. Pittendrigh, C.S., and Minis, D.H. (1972). Circadian systems: longevity as a function of circadian resonance in Drosophila melanogaster. Proc. Natl. Acad. Sci. USA *69*, 1537–1539.
2. Zheng, X., and Sehgal, A. (2012). Speed control: cogs and gears that drive the circadian clock. Trends. Neurosci. *35*, 574–585.
3. Patke, A., Young, M.W., and Axelrod, S. (2020). Molecular mechanisms and physiological importance of circadian rhythms. Nat. Rev. Mol. Cell. Biol. *21*, 67–84.
4. Lee, C., Bae, K., and Edery, I. (1999). PER and TIM inhibit the DNA binding activity of a Drosophila CLOCK-CYC/dBMAL1 heterodimer without disrupting formation of the heterodimer: a basis for circadian transcription. Mol. Cell Biol. *19*, 5316–5325.
5. Menet, J.S., Abruzzi, K.C., Desrochers, J., Rodriguez, J., and Rosbash, M. (2010). Dynamic PER repression mechanisms in the Drosophila circadian clock: from on-DNA to off-DNA. Genes. Dev. *24*, 358–367.
6. Cyran, S.A., Buchsbaum, A.M., Reddy, K.L., Lin, M.-C., Glossop, N.R.J., Hardin, P.E., Young, M.W., Storti, R.V., and Blau, J. (2003). vrille, Pdp1, and dClock form a second feedback loop in the Drosophila circadian clock. Cellule *112*, 329–341.
7. Glossop, N.R.J., Houl, J.H., Zheng, H., Ng, F.S., Dudek, S.M., and Hardin, P.E. (2003). VRILLE feeds back to control circadian transcription of Clock in the Drosophila circadian oscillator. Neuron *37*, 249–261.
8. Kadener, S., Stoleru, D., McDonald, M., Nawathean, P., and Rosbash, M. (2007). Clockwork Orange is a transcriptional repressor and a new Drosophila circadian pacemaker component. Genes Dev. *21*, 1675–1686.
9. Lim, C., Chung, B.Y., Pitman, J.L., McGill, J.J., Pradhan, S., Lee, J., Keegan, K.P., Choe, J., and Allada, R. (2007). Clockwork orange encodes a transcriptional repressor important for circadian-clock amplitude in Drosophila. Curr. Biol. *17*, 1082–1089.
10. Richier, B., Michard-Vanhée, C., Lamouroux, A., Papin, C., and Rouyer, F. (2008). The clockwork orange Drosophila protein functions as both an activator and a repressor of clock gene expression. J. Biol. Rhythm. *23*, 103–116.
11. Zhou, J., Yu, W., and Hardin, P.E. (2016). CLOCKWORK ORANGE enhances PERIOD mediated rhythms in transcriptional repression by antagonizing E-box binding by CLOCK-CYCLE. PLoS Genet. *12*, e1006430.
12. Edery, I., Zwiebel, L.J., Dembinska, M.E., and Rosbash, M. (1994). Temporal phosphorylation of the Drosophila period protein. Proc. Natl. Acad. Sci. USA *91*, 2260–2264.
13. Price, J.L., Blau, J., Rothenfluh, A., Abodeely, M., Kloss, B., and Young, M.W. (1998). double-time is a novel Drosophila clock gene that regulates PERIOD protein accumulation. Cell *94*, 83–95.
14. Chiu, J.C., Ko, H.W., and Edery, I. (2011). NEMO/NLK phosphorylates PERIOD to initiate a time-delay phosphorylation circuit that sets circadian clock speed. Cell *145*, 357–370.
15. Grima, B., Lamouroux, A., Chélot, E., Papin, C., Limbourg-Bouchon, B., and Rouyer, F. (2002). The F-box protein slimb controls the levels of clock proteins period and timeless. Nature *420*, 178–182.
16. Ko, H.W., Jiang, J., and Edery, I. (2002). Role for Slimb in the degradation of Drosophila Period protein phosphorylated by Doubletime. Nature *420*, 673–678.
17. Chiu, J.C., Vanselow, J.T., Kramer, A., and Edery, I. (2008). The phosphooccupancy of an atypical SLIMB-binding site on PERIOD that is phosphorylated by DOUBLETIME controls the pace of the clock. Genes Dev. *22*, 1758–1772.
18. Schmid, F.X. (1993). Prolyl isomerase: enzymatic catalysis of slow protein-folding reactions. Annu. Rev. Biophys. Biomol. Struct. *22*, 123–142.

19. Fischer, G., Wittmann-Liebold, B., Lang, K., Kiefhaber, T., and Schmid, F. X. (1989). Cyclophilin and peptidyl-prolyl cis-trans isomerase are probably identical proteins. Nature *337*, 476–478.

20. Siekierka, J.J., Hung, S.H., Poe, M., Lin, C.S., and Sigal, N.H. (1989). A cytosolic binding protein for the immunosuppressant FK506 has peptidyl-prolyl isomerase activity but is distinct from cyclophilin. Nature *341*, 755–757.

21. Rahfeld, J.-U., Schierhorn, A., Mann, K., and Fischer, G. (1994). A novel peptidyl-prolyl cisltrans isomerase from Escherichia coli. FEBS. Lett. *343*, 65–69.

22. Jordens, J., Janssens, V., Longin, S., Stevens, I., Martens, E., Bultynck, G., Engelborghs, Y., Lescrinier, E., Waelkens, E., Goris, J., and Van Hoof, C. (2006). The protein phosphatase 2A phosphatase activator is a novel peptidyl-prolyl cis/trans-isomerase. J. Biol. Chem. *281*, 6349–6357.

23. Lu, K.P., Finn, G., Lee, T.H., and Nicholson, L.K. (2007). Prolyl cis-trans isomerization as a molecular timer. Nat. Chem. Biol. *3*, 619–629.

24. Hanes, S.D. (2015). Prolyl isomerases in gene transcription. Biochim. Biophys. Acta *1850*, 2017–2034.

25. Wang, L., Zhou, Y., Chen, D., and Lee, T.H. (2020). Peptidyl-prolyl cis/trans isomerase Pin1 and Alzheimer's disease. Front. Cell Dev. Biol. *8*, 355.

26. Theuerkorn, M., Fischer, G., and Schiene-Fischer, C. (2011). Prolyl cis/trans isomerase signalling pathways in cancer. Curr. Opin. Pharmacol. *11*, 281–287.

27. Stifani, S. (2018). The multiple roles of peptidyl prolyl isomerases in brain cancer. Biomolecules *8*, 112.

28. Rostam, M.A., Piva, T.J., Rezaei, H.B., Kamato, D., Little, P.J., Zheng, W., and Osman, N. (2015). Peptidyl-prolyl isomerases: functionality and potential therapeutic targets in cardiovascular disease. Clin. Exp. Pharmacol. Physiol. *42*, 117–124.

29. Kanna, M., Nakatsu, Y., Yamamotoya, T., Encinas, J., Ito, H., Okabe, T., Asano, T., and Sakaguchi, T. (2022). Roles of peptidyl prolyl isomerase Pin1 in viral propagation. Front. Cell Dev. Biol. *10*, 1005325.

30. Mamatis, J.E., Pellizzari-Delano, I.E., Gallardo-Flores, C.E., and Colpitts, C.C. (2022). Emerging roles of cyclophilin A in regulating viral cloaking. Front. Microbiol. *13*, 828078.

31. Kang, S.W., Lee, E., Cho, E., Seo, J.H., Ko, H.W., and Kim, E.Y. (2015). Drosophila peptidyl-prolyl isomerase Pin1 modulates circadian rhythms via regulating levels of PERIOD. Biochem. Biophys. Res. Commun. *463*, 235–240.

32. Gustafson, C.L., Parsley, N.C., Asimgil, H., Lee, H.-W., Ahlbach, C., Michael, A.K., Xu, H., Williams, O.L., Davis, T.L., Liu, A.C., and Partch, C.L. (2017). A slow conformational switch in the BMAL1 transactivation domain modulates circadian rhythms. Mol. Cell *66*, 447–457.e7.

33. Green, E.W., Fedele, G., Giorgini, F., and Kyriacou, C.P. (2014). A Drosophila RNAi collection is subject to dominant phenotypic effects. Nat. Methods *11*, 222–223.

34. Vissers, J.H.A., Manning, S.A., Kulkarni, A., and Harvey, K.F. (2016). A Drosophila RNAi library modulates Hippo pathway-dependent tissue growth. Nat. Commun. *7*, 10368.

35. Foley, L.E., Ling, J., Joshi, R., Evantal, N., Kadener, S., and Emery, P. (2019). Drosophila PSI controls circadian period and the phase of circadian behavior under temperature cycle via tim splicing. Elife *8*, e50063.

36. Renn, S.C., Park, J.H., Rosbash, M., Hall, J.C., and Taghert, P.H. (1999). A pdf neuropeptide gene mutation and ablation of PDF neurons each cause severe abnormalities of behavioral circadian rhythms in Drosophila. Cell *99*, 791–802.

37. Grima, B., Chélot, E., Xia, R., and Rouyer, F. (2004). Morning and evening peaks of activity rely on different clock neurons of the Drosophila brain. Nature *431*, 869–873.

38. Stoleru, D., Peng, Y., Agosto, J., and Rosbash, M. (2004). Coupled oscillators control morning and evening locomotor behaviour of Drosophila. Nature *431*, 862–868.

39. Stoleru, D., Nawathean, P., Fernández, M.d.l.P., Menet, J.S., Ceriani, M. F., and Rosbash, M. (2007). The Drosophila circadian network is a seasonal timer. Cell *129*, 207–219.

40. Hunter-Ensor, M., Ousley, A., and Sehgal, A. (1996). Regulation of the Drosophila protein timeless suggests a mechanism for resetting the circadian clock by light. Cell *84*, 677–685.

41. Myers, M.P., Wager-Smith, K., Rothenfluh-Hilfiker, A., and Young, M.W. (1996). Light-induced degradation of TIMELESS and entrainment of the Drosophila circadian clock. Science *271*, 1736–1740.

42. Hamblen, M., Zehring, W.A., Kyriacou, C.P., Reddy, P., Yu, Q., Wheeler, D. A., Zwiebel, L.J., Konopka, R.J., Rosbash, M., and Hall, J.C. (1986). Germline transformation involving DNA from the period locus in Drosophila melanogaster: overlapping genomic fragments that restore circadian and ultradian rhythmicity to per0 and per− mutants. J. Neurogenet. *3*, 249–291.

43. Frisch, B., Hardin, P.E., Hamblen-Coyle, M.J., Rosbash, M., and Hall, J.C. (1994). A promoterless period gene mediates behavioral rhythmicity and cyclical per expression in a restricted subset of the Drosophila nervous system. Neuron *12*, 555–570.

44. So, W.V., and Rosbash, M. (1997). Post-transcriptional regulation contributes to Drosophila clock gene mRNA cycling. EMBO J. *16*, 7146–7155.

45. Kim, E.Y., Ko, H.W., Yu, W., Hardin, P.E., and Edery, I. (2007). A DOUBLETIME kinase binding domain on the Drosophila PERIOD protein is essential for its hyperphosphorylation, transcriptional repression, and circadian clock function. Mol. Cell Biol. *27*, 5014–5028.

46. Yang, Z., and Sehgal, A. (2001). Role of molecular oscillations in generating behavioral rhythms in Drosophila. Neuron *29*, 453–467.

47. Gullerova, M., Barta, A., and LORKOVIĆ, Z.J. (2006). AtCyp59 is a multidomain cyclophilin from Arabidopsis thaliana that interacts with SR proteins and the C-terminal domain of the RNA polymerase II. RNA *12*, 631–643.

48. Gullerova, M., Barta, A., and Lorkovic, Z.J. (2007). Rct1, a nuclear RNA recognition motif-containing cyclophilin, regulates phosphorylation of the RNA polymerase II C-terminal domain. Mol. Cell Biol. *27*, 3601–3611.

49. Bannikova, O., Zywicki, M., Marquez, Y., Skrahina, T., Kalyna, M., and Barta, A. (2013). Identification of RNA targets for the nuclear multidomain cyclophilin atCyp59 and their effect on PPIase activity. Nucleic. Acids. Res. *41*, 1783–1796.

50. Ahn, J.H., Rechsteiner, A., Strome, S., and Kelly, W.G. (2016). A conserved nuclear cyclophilin is required for both RNA polymerase II elongation and cotranscriptional splicing in Caenorhabditis elegans. PLoS Genet. *12*, e1006227.

51. Aoyagi, N., and Wassarman, D.A. (2000). Genes encoding Drosophila melanogaster RNA polymerase II general transcription factors: diversity in TFIIA and TFIID components contributes to gene-specific transcriptional regulation. J. Cell. Biol. *150*, F45–F50.

52. Wild, T., and Cramer, P. (2012). Biogenesis of multisubunit RNA polymerases. Trends Biochem. Sci. *37*, 99–105.

53. Phatnani, H.P., and Greenleaf, A.L. (2006). Phosphorylation and functions of the RNA polymerase II CTD. Genes Dev. *20*, 2922–2936.

54. Gibbs, E.B., Lu, F., Portz, B., Fisher, M.J., Medellin, B.P., Laremore, T.N., Zhang, Y.J., Gilmour, D.S., and Showalter, S.A. (2017). Phosphorylation induces sequence-specific conformational switches in the RNA polymerase II C-terminal domain. Nat. Commun. *8*, 15233.

55. Hsin, J.-P., and Manley, J.L. (2012). The RNA polymerase II CTD coordinates transcription and RNA processing. Genes Dev. *26*, 2119–2137.

56. Zaborowska, J., Egloff, S., and Murphy, S. (2016). The pol II CTD: new twists in the tail. Nat. Struct. Mol. Biol. *23*, 771–777.

57. Harlen, K.M., and Churchman, L.S. (2017). The code and beyond: transcription regulation by the RNA polymerase II carboxy-terminal domain. Nat. Rev. Mol. Cell Biol. *18*, 263–273.

58. Miyao, T., and Woychik, N.A. (1998). RNA polymerase subunit RPB5 plays a role in transcriptional activation. Proc. Natl. Acad. Sci. USA *95*, 15281–15286.

59. Ishiguro, A., Nogi, Y., Hisatake, K., Muramatsu, M., and Ishihama, A. (2000). The Rpb6 subunit of fission yeast RNA polymerase II is a contact target of the transcription elongation factor TFIIS. Mol. Cell Biol. *20*, 1263–1270.

60. Martinez-Fernandez, V., Garrido-Godino, A.I., Mirón-García, M.C., Begley, V., Fernandez-Pevida, A., de la Cruz, J., Chavez, S., and Navarro, F.

(2018). Rpb5 modulates the RNA polymerase II transition from initiation to elongation by influencing Spt5 association and backtracking. Biochimica et Biophysica Acta (BBA)-Gene Regulatory Mechanisms *1861*, 1–13.

61. Fujiyama-Nakamura, S., Ito, S., Sawatsubashi, S., Yamauchi, Y., Suzuki, E., Tanabe, M., Kimura, S., Murata, T., Isobe, T., and Ichi Takeyama, K. (2009). BTB protein, dKLHL18/CG3571, serves as an adaptor subunit for a dCul3 ubiquitin ligase complex. Genes Cells *14*, 965–973.
62. Herold, N., Will, C.L., Wolf, E., Kastner, B., Urlaub, H., and Lührmann, R. (2009). Conservation of the protein composition and electron microscopy structure of Drosophila melanogaster and human spliceosomal complexes. Mol. Cell Biol. *29*, 281–301.
63. Jiang, J., and Struhl, G. (1998). Regulation of the Hedgehog and Wingless signalling pathways by the F-box/WD40-repeat protein Slimb. Nature *391*, 493–496.
64. Ho, M.S., Tsai, P.-I., and Chien, C.-T. (2006). F-box proteins: the key to protein degradation. J. Biomed. Sci. *13*, 181–191.
65. Liu, W., Ma, Q., Wong, K., Li, W., Ohgi, K., Zhang, J., Aggarwal, A., and Rosenfeld, M.G. (2013). Brd4 and JMJD6-associated anti-pause enhancers in regulation of transcriptional pause release. Cell *155*, 1581–1595.
66. Barak, T., Ristori, E., Ercan-Sencicek, A.G., Miyagishima, D.F., Nelson-Williams, C., Dong, W., Jin, S.C., Prendergast, A., Armero, W., Henegariu, O., et al. (2021). PPIL4 is essential for brain angiogenesis and implicated in intracranial aneurysms in humans. Nat. Med. *27*, 2165–2175.
67. Thapar, R. (2015). Roles of prolyl isomerases in RNA-mediated gene expression. Biomolecules *5*, 974–999.
68. Zhou, Z., Licklider, L.J., Gygi, S.P., and Reed, R. (2002). Comprehensive proteomic analysis of the human spliceosome. Nature *419*, 182–185.
69. Hegele, A., Kamburov, A., Grossmann, A., Sourlis, C., Wowro, S., Weimann, M., Will, C.L., Pena, V., Lührmann, R., and Stelzl, U. (2012). Dynamic protein-protein interaction wiring of the human spliceosome. Mol. Cell. *45*, 567–580.
70. Kanin, E.I., Kipp, R.T., Kung, C., Slattery, M., Viale, A., Hahn, S., Shokat, K. M., and Ansari, A.Z. (2007). Chemical inhibition of the TFIIH-associated kinase Cdk7/Kin28 does not impair global mRNA synthesis. Proc. Natl. Acad. Sci. USA *104*, 5812–5817.
71. Hong, S.W., Hong, S.M., Yoo, J.W., Lee, Y.C., Kim, S., Lis, J.T., and Lee, D-k (2009). Phosphorylation of the RNA polymerase II C-terminal domain by TFIIH kinase is not essential for transcription of Saccharomyces cerevisiae genome. Proc. Natl. Acad. Sci. USA *106*, 14276–14280.
72. Kim, H., Erickson, B., Luo, W., Seward, D., Graber, J.H., Pollock, D.D., Megee, P.C., and Bentley, D.L. (2010). Gene-specific RNA polymerase II phosphorylation and the CTD code. Nat. Struct. Mol. Biol. *17*, 1279–1286.
73. Blazek, D., Kohoutek, J., Bartholomeeusen, K., Johansen, E., Hulinkova, P., Luo, Z., Cimermancic, P., Ule, J., and Peterlin, B.M. (2011). The Cyclin K/Cdk12 complex maintains genomic stability via regulation of expression of DNA damage response genes. Genes Dev. *25*, 2158–2172.
74. Lu, H., Zawel, L., Fisher, L., Egly, J.-M., and Reinberg, D. (1992). Human general transcription factor IIH phosphorylates the C-terminal domain of RNA polymerase II. Nature *358*, 641–645.
75. Schwartz, B.E., Larochelle, S., Suter, B., and Lis, J.T. (2003). Cdk7 is required for full activation of Drosophila heat shock genes and RNA polymerase II phosphorylation in vivo. Mol. Cell Biol. *23*, 6876–6886.
76. Krishnamurthy, S., He, X., Reyes-Reyes, M., Moore, C., and Hampsey, M. (2004). Ssu72 Is an RNA polymerase II CTD phosphatase. Mol. Cell *14*, 387–394.
77. Lee, C., Bae, K., and Edery, I. (1998). The Drosophila CLOCK protein undergoes daily rhythms in abundance, phosphorylation, and interactions with the PER–TIM complex. Neuron *21*, 857–867.
78. Saifee, N.H., and Zheng, N. (2008). A ubiquitin-like protein unleashes ubiquitin ligases. Cell *135*, 209–211.
79. Sarikas, A., Hartmann, T., and Pan, Z.-Q. (2011). The cullin protein family. Genome. Biol. *12*, 220.
80. Voigt, J., and Papalopulu, N. (2006). A dominant-negative form of the E3 ubiquitin ligase Cullin-1 disrupts the correct allocation of cell fate in the neural crest lineage. Development *133*, 559–568.
81. Abbas, T., Mueller, A.C., Shibata, E., Keaton, M., Rossi, M., and Dutta, A. (2013). CRL1-FBXO11 promotes Cdt2 ubiquitylation and degradation and regulates Pr-Set7/Set8-mediated cellular migration. Mol. Cell *49*, 1147–1158.
82. Koh, K., Zheng, X., and Sehgal, A. (2006). JETLAG resets the Drosophila circadian clock by promoting light-induced degradation of TIMELESS. Science *312*, 1809–1812.
83. Grima, B., Dognon, A., Lamouroux, A., Chélot, E., and Rouyer, F. (2012). CULLIN-3 controls TIMELESS oscillations in the Drosophila circadian clock. PLoS Biol. *10*, e1001367.
84. Kim, E.Y., Jeong, E.H., Park, S., Jeong, H.-J., Edery, I., and Cho, J.W. (2012). A role for O-GlcNAcylation in setting circadian clock speed. Genes Dev. *26*, 490–502.
85. Lee, E., Cho, E., Kang, D.H., Jeong, E.H., Chen, Z., Yoo, S.-H., and Kim, E. Y. (2016). Pacemaker-neuron–dependent disturbance of the molecular clockwork by a Drosophila CLOCK mutant homologous to the mouse Clock mutation. Proc. Natl. Acad. Sci. USA *113*, E4904–E4913.
86. Lee, S.H., Cho, E., Yoon, S.-E., Kim, Y., and Kim, E.Y. (2021). Metabolic control of daily locomotor activity mediated by tachykinin in Drosophila. Commun. Biol. *4*, 693.
87. Wu, G., Anafi, R.C., Hughes, M.E., Kornacker, K., and Hogenesch, J.B. (2016). MetaCycle: an integrated R package to evaluate periodicity in large scale data. Bioinformatics *32*, 3351–3353. https://doi.org/10.1093/bioinformatics/btw405.
88. Venken, K.J., He, Y., Hoskins, R.A., and Bellen, H.J. (2006). P [acman]: a BAC transgenic platform for targeted insertion of large DNA fragments in D. melanogaster. Science *314*, 1747–1751.
89. Groth, A.C., Fish, M., Nusse, R., and Calos, M.P. (2004). Construction of transgenic Drosophila by using the site-specific integrase from phage φC31. Genetics *166*, 1775–1782.
90. Schmid, B., Helfrich-Förster, C., and Yoshii, T. (2011). A new ImageJ plug-in "ActogramJ" for chronobiological analyses. J. Biol. Rhythm. *26*, 464–467.
91. Kim, E.Y., and Edery, I. (2006). Balance between DBT/CKIε kinase and protein phosphatase activities regulate phosphorylation and stability of Drosophila CLOCK protein. Proc. Natl. Acad. Sci. USA *103*, 6178–6183.
92. Gunawardhana, K.L., and Hardin, P.E. (2017). VRILLE controls PDF neuropeptide accumulation and arborization rhythms in small ventrolateral neurons to drive rhythmic behavior in Drosophila. Curr. Biol. *27*, 3442–3453.e4.
93. Dobin, A., Davis, C.A., Schlesinger, F., Drenkow, J., Zaleski, C., Jha, S., Batut, P., Chaisson, M., and Gingeras, T.R. (2013). STAR: ultrafast universal RNA-seq aligner. Bioinformatics *29*, 15–21.
94. Li, B., and Dewey, C.N. (2011). RSEM: accurate transcript quantification from RNA-Seq data with or without a reference genome. BMC. Bioinformatics. *12*, 323.
95. Love, M.I., Huber, W., and Anders, S. (2014). Moderated estimation of fold change and dispersion for RNA-seq data with DESeq2. Genome Biol. *15*, 550.
96. Anders, S., Reyes, A., and Huber, W. (2012). Detecting differential usage of exons from RNA-seq data. Genome. Res. *22*, 2008–2017.
97. Lawrence, M., Huber, W., Pagès, H., Aboyoun, P., Carlson, M., Gentleman, R., Morgan, M.T., and Carey, V.J. (2013). Software for computing and annotating genomic ranges. PLoS Comput. Biol. *9*, e1003118.

STAR★METHODS

KEY RESOURCES TABLE

REAGENT or RESOURCE	SOURCE	IDENTIFIER
Antibodies		
Rabbit anti-PER	Kim et al.[84]	N/A
Rabbit anti-TIM	Lee et al.[85]	N/A
Guinea pig anti-CLK	Lee et al.[86]	N/A
Guinea pig anti-VRI	Gift from Paul E. Hardin[6]	N/A
Mouse anti-PDF (C7)	Developmental Studies Hybridoma Bank	RRID: AB_760350
Mouse Anti-nc82	Developmental Studies Hybridoma Bank	RRID: AB_2314866
Guinea pig anti-dPPIL4 (Gp1)	This journal	N/A
Guinea pig anti-dPPIL4 (Gp2)	This journal	N/A
Rabbit anti-RNApol II CTD-pSer2	Abcam	Cat# ab5095, RRID: AB_304749
Mouse anti-RNApol II CTD-pSer5	Abcam	Cat# ab5408, RRID: AB_304868
Mouse anti-RNApol II CTD-Total	Millipore	Cat# CBL221, RRID: AB_2167489
Rabbit anti-CUL1	Thermo Fisher Scientific	Cat# 71-8700, RRID: AB_2534002
Rat anti-Ci	Developmental Studies Hybridoma Bank	Cat# 2A1, RRID: AB_2109711
Mouse anti-β-Tubulin (E7)	Developmental Studies Hybridoma Bank	RRID: AB_528499
Rabbit anti-Actin	Sigma-Aldrich	Cat# A2066, RRID: AB_476693
Rabbit anti-OGT	Santa Cruz Biotechnology	Cat# sc-32921, RRID: AB_2156938
Goat anti-Rabbit HRP	Thermo Fisher Scientific	Cat# G-21234, RRID:AB_2536530
Goat anti-Mouse HRP	Thermo Fisher Scientific	Cat# G-21040, RRID:AB_2536527
Goat anti-Guinea pig HRP	Abcam	Cat# ab6908, RRID:AB_955425
Goat anti-Rabbit Alexa Flour 488	Thermo Fisher Scientific	Cat# A-11008, RRID:AB_143165
Goat anti-Rabbit Alexa Flour 555	Thermo Fisher Scientific	Cat# A-21428, RRID:AB_2535849
Goat anti-Mouse Alexa Flour 555	Thermo Fisher Scientific	Cat# A-21424, RRID:AB_141780
Goat anti-Mouse Alexa Flour 633	Thermo Fisher Scientific	Cat# A-21050, RRID:AB_2535718
Goat anti-Guinea pig Alexa Flour 488	Thermo Fisher Scientific	Cat# A-11073, RRID:AB_2534117
Experimental models: Organisms/strains		
Drosophila/*dcr2*;*tim*(UAS)-Gal4	Kim et al.[84]	N/A
Drosophila/*tub*-Gal80ts;*tim*(UAS)-Gal4	Kim et al.[84]	N/A
Drosophila/$wper^{0}$;*dcr2*;*tim*(UAS)-Gal4	This journal	N/A
Drosophila/$wper^{0}$;;*per*(wt-13.2HAHis), M16	Kim et al.[45]	N/A
Drosophila/per^{01};;*per7.2:9*	Gift from Paul E. Hardin[42,43]	N/A
Drosophila/UAS-*dppil4*-V5	This journal	N/A
Drosophila/$dppil4^{ex81}$	This journal	N/A
Drosophila/$dppil4^{ex88}$	This journal	N/A
Drosophila/$dppil4^{ex170}$	This journal	N/A
Drosophila/w^{1118}	Bloomington Drosophila Stock Center	RRID: BDSC 5905
Drosophila/*yw* per^{01}	Bloomington Drosophila Stock Center	RRID: BDSC 80917
Drosophila/UAS-CG5808 Ri (Trip)	Bloomington Drosophila Stock Center	RRID: BDSC 55208
Drosophila/UAS-GFP.nls	Bloomington Drosophila Stock Center	RRID: BDSC 4776
Drosophila/*w**;P(UAS-*per*.Y)3-1	Bloomington Drosophila Stock Center	RRID: BDSC 80685
Drosophila/UAS-*Fkbp12* Ri-1	Vienna Drosophila Resource center	VDRC 45015
Drosophila/UAS-*Fkbp14* Ri-1	Vienna Drosophila Resource center	VDRC 101932
Drosophila/UAS-*CG5071* Ri-1	Vienna Drosophila Resource center	VDRC 12863
Drosophila/UAS-*Cyp40* Ri	Vienna Drosophila Resource center	VDRC 45986

(*Continued on next page*)

Continued

REAGENT or RESOURCE	SOURCE	IDENTIFIER
Drosophila/UAS-*Fkbp14* Ri-2	Vienna Drosophila Resource center	VDRC 23729
Drosophila/UAS-*CG11858* Ri	Vienna Drosophila Resource center	VDRC 39071
Drosophila/UAS-*CG17266* Ri	Vienna Drosophila Resource center	VDRC 110097
Drosophila/UAS-*Cyp1* Ri	Vienna Drosophila Resource center	VDRC 12828
Drosophila/UAS-*CG14715* Ri	Vienna Drosophila Resource center	VDRC 104005
Drosophila/UAS-*CG5071* Ri-2	Vienna Drosophila Resource center	VDRC 34925
Drosophila/UAS-*Fkbp39* Ri	Vienna Drosophila Resource center	VDRC 103035
Drosophila/UAS-*CG11777* Ri	Vienna Drosophila Resource center	VDRC 104435
Drosophila/UAS-*CG2852* Ri	Vienna Drosophila Resource center	VDRC 20669
Drosophila/UAS-*shu* Ri	Vienna Drosophila Resource center	VDRC 15069
Drosophila/UAS-*Fkbp12* Ri-2	Vienna Drosophila Resource center	VDRC 105832
Drosophila/UAS-*Moca-cyp* Ri-1	Vienna Drosophila Resource center	VDRC 45014
Drosophila/UAS-*Moca-cyp* Ri-2	Vienna Drosophila Resource center	VDRC 20670
Drosophila/UAS-*CG3511* Ri-1	Vienna Drosophila Resource center	VDRC 21863
Drosophila/UAS-*Fkbp59* Ri	Vienna Drosophila Resource center	VDRC 21735
Drosophila/UAS-*dod* Ri-1	Vienna Drosophila Resource center	VDRC 25209
Drosophila/UAS-*dod* Ri-2	Vienna Drosophila Resource center	VDRC 25210
Drosophila/UAS-*cyp33* Ri	Vienna Drosophila Resource center	VDRC 108734
Drosophila/UAS-*Cypl* Ri	Vienna Drosophila Resource center	VDRC 104316
Drosophila/UAS-*CG5808* Ri-2	Vienna Drosophila Resource center	VDRC 22199
Drosophila/UAS-*CG3511* Ri-2	Vienna Drosophila Resource center	VDRC 110015
Drosophila/UAS-*CG7747* Ri	Vienna Drosophila Resource center	VDRC 105644
Drosophila/UAS-*CG10907* Ri	Vienna Drosophila Resource center	VDRC 103623
Drosophila/UAS-*CG7768* Ri	Vienna Drosophila Resource center	VDRC 109900
Drosophila/UAS-*CG5808* Ri-1	Vienna Drosophila Resource center	VDRC 103789
Drosophila/40D-UAS	Vienna Drosophila Resource center	VDRC 60101
Drosophila/UAS-*Polr2A* Ri	Vienna Drosophila Resource center	VDRC 110340
Drosophila/UAS-*Polr2E* Ri	Vienna Drosophila Resource center	VDRC 105248
Drosophila/UAS-*Polr2F* Ri	Vienna Drosophila Resource center	VDRC 105937
Drosophila/UAS-*Polr2H* Ri	Vienna Drosophila Resource center	VDRC 106838
Chemicals		
Pierce™ Protein A Magnetic Beads	Thermo Fisher Scientific	Cat# 88845
Formaldehyde	Thermo Fisher Scientific	Cat# 28906
QIAzol	Qiagen	Cat# 79306
TB Green Premix Ex Taq	TaKaRa	Cat# RR420A
Cycloheximide	Sigma-Aldrich	Cat# C7698
Oligonucleotides		
dppil4 mRNA forward 5'-TTAGTAGCTTCGGCGTGCTT-3'	Macrogen	N/A
dppil4 mRNA reverse 5'-CTTTGAAACGGATTGGGAGA-3'	Macrogen	N/A
per mRNA forward 5'-GACCGAATCCCTGCTCAATA-3'	Macrogen	N/A
per mRNA reverse 5'-GTGTCATTGGCGGACTTCTT-3'	Macrogen	N/A
per pre-mRNA forward 5'-GTGAGAGCGAGAGCGAGTGT-3'	Macrogen	N/A
per pre-mRNA reverse 5'-TATGTAAGCTGCCTGCCCAA-3'	Macrogen	N/A

(*Continued on next page*)

Continued

REAGENT or RESOURCE	SOURCE	IDENTIFIER
tim mRNA forward 5'-TGATCGAGTTGCAGTGCTTC-3'	Macrogen	N/A
tim mRNA reverse 5'-CCCTTATACCCGAGGTGGAT-3'	Macrogen	N/A
tim pre-mRNA forward 5'-GTTTCGGTCAGTGTGTGTATCT-3'	Macrogen	N/A
tim pre-mRNA reverse 5'-GCTCAACGAACCGCTTACT-3'	Macrogen	N/A
cbp20 forward 5′-GTATAAGAAGACGCCCTGC-3′	Macrogen	N/A
cbp20 reverse 5′-TTCACAAATCTCATGGCCG-3′	Macrogen	N/A
Software and algorithms		
Drosophila Activity Monitoring System 3	Trikinetics	N/A
FaasX	Trikinetics	N/A
Image J	Image J	N/A
Rotor-Gene Q-Pure Detection	Qiagen	N/A
Zen	Carl Zeiss	N/A
Prism9	GraphPad	N/A
Metacycle	Wu et al.[87]; https://CRAN.R-project.org/package=MetaCycle	RRID: SCR_025729
Deposited data		
RNA-seq data	This paper	GSE292592

EXPERIMENTAL MODEL AND STUDY PARTICIPANT DETAILS

Fly stocks

dcr2;*tim*(UAS)-Gal,[84] *tub*-Gal80^{ts};*tim*(UAS)-Gal,[84] and *dcr2*;*tim*(UAS)-Gal4 were crossed with *yw per*^{01} to generate *wper*^{0};*dcr2*;*tim*(UAS)-Gal4 flies. *wper*^{0};;*per*(wt-13.2HAHis), M16 was described previousl.[45] *per*^{01};;*per7.2:9* flies were a gift from Paul E. Hardin (Texas A&M University, USA).[42,43] The following lines were obtained from the Bloomington Drosophila Stock Center: *w*^{1118} (BL5905), UAS-*CG5808* Ri (BL55208), UAS-GFP.nls (BL4776), and *w**;P(UAS-*per*.Y)3-1 (BL80685).[46] The following fly stocks were obtained from the Vienna Drosophila Resource Center: UAS-*Fkbp12* Ri-1 (VDRC45015), UAS-*Fkbp14* Ri-1 (VDRC101932), UAS-*CG5071* Ri-1 (VDRC12863), UAS-*Cyp40* Ri (VDRC45986), UAS-*Fkbp14* Ri-2 (VDRC23729), UAS-*CG11858* Ri (VDRC39071), UAS-*CG17266* Ri (VDRC110097), UAS-*Cyp1* Ri (VDRC12828), UAS-*CG14715* Ri (VDRC104005), UAS-*CG5071* Ri-2 (VDRC34925), UAS-*Fkbp39* Ri (VDRC103035), UAS-*CG11777* Ri (VDRC104435), UAS-*CG2852* Ri (VDRC20669), UAS-*shu* Ri (VDRC15069), UAS-*Fkbp12* Ri-2 (VDRC105832), UAS-*Moca-cyp* Ri-1 (VDRC45014), UAS-*Moca-cyp* Ri-2 (VDRC20670), UAS-*CG3511* Ri-1 (VDRC21863), UAS-*Fkbp59* Ri (VDRC21735), UAS-*dod* Ri-1 (VDRC25209), UAS-*dod* Ri-2 (VDRC25210), UAS-*cyp33* Ri (VDRC108734), UAS-*Cypl* Ri (VDRC104316), UAS-*CG5808* Ri-2 (VDRC22199), UAS-*CG3511* Ri-2 (VDRC110015), UAS-*CG7747* Ri (VDRC105644), UAS-*CG10907* Ri (VDRC103623), UAS-*CG7768* Ri (VDRC109900), UAS-*CG5808* Ri-1 (VDRC103789), 40D-UAS (VDRC60101), UAS-*Polr2A* Ri (VDRC110340), UAS-*Polr2E* Ri (VDRC105248), UAS-*Polr2F* Ri (VDRC105937), and UAS-*Polr2H* Ri (VDRC 106838).

Transgenic fly generation

To generate transgenic flies harboring pUAST-*dppil4* (*CG5808*)-V5, full-length *dppil4* (*CG5808*) cDNA was amplified by PCR using the Drosophila Genomics Resource Center clone GH01073 (RRID: DGRC_5607) as a template, and the product was subcloned into the pUAST vector via EcoRI and NotI digestion. *PhiC31* integrase-mediated transgenesis was used to insert the pUAST-*dppil4* (*CG5808*)-V5 plasmid into the VK00018 attP site on chromosome 2 (BestGene Inc.).[88,89] We employed P element excision mutagenesis to generate a *dppil4* (*CG5808)*-null allele. A fly line harboring the P element near the *dppil4* (*CG5808*) gene, *P{Epgy2}CG5808*^{EY13836}, was mated to *Dr/TM3,p{Δ2-3}* flies. Two fly lines harboring a precisely excised chromosome (control) and three fly lines harboring small and large deletions, named *dppil4*^{ex81}, *dppil4*^{ex88}, and *dppil4*^{ex170} were obtained. The primer sequences used for genomic DNA PCR were as follows: primer-1-forward, 5'-TCGCGCCCGGCACAATCAAGT-3'; primer-2-reverse, 5'-GCGCCGAATGTGCTGACCACTGTA-3'. The precision of deleted regions was confirmed by sequencing.

METHOD DETAILS

Locomotor behavior analysis

The locomotor activity of individual flies was determined using Drosophila Activity Monitoring System 3 software (Trikinetics, version 1.02). 2-5 days old male flies were used for the analysis and maintained in glass tubes containing 2% agar and 5% sucrose. The flies were exposed to 12 h of light and 12 h of dark (LD) for 4 days and then were maintained in constant darkness (DD) for 7 days at 25°C. The locomotor data analysis was performed using FaasX software (Fly Activity Analysis Suite for MacOSX), which was generously provided by Francois Rouyer (Centre National de la Recherche Scientifique, France). Periods were calculated for each fly using χ^2 periodogram analysis, and data were pooled to obtain an average value. The power was calculated by quantifying the relative strength of the rhythm during the DD condition. Individual flies with a power $\geq$10 and width $\geq$2 were considered rhythmic. Actograms represent the double-plotted locomotor activities throughout the experimental period and were acquired using Actogram J software.[90]

Western blotting and immunoprecipitation

We produced guinea pig anti-dPPIL4 antiserum (Gp1 and Gp2) using the N-terminal amino acids (1–550) of the protein as an antigen (Young In Frontier Co. Ltd.). We verified that Gp1 and Gp2 antiserum specifically recognized dPPIL4 proteins in *Drosophila* S2 cells and flies (Figure S3). Gp1 antiserum was mainly used for immunoprecipitation, and Gp2 antiserum was used for western blotting.

For western blotting, protein extracts were prepared in radioimmunoprecipitation assay (RIPA) lysis buffer [25 mM Tris-HCl, pH7.5, 50 mM NaCl, 0.5% sodium deoxycholate, 0.5% NP-40, and 0.1% sodium dodecyl sulfate (SDS)] with a freshly added protease and phosphatase inhibitor mixture (Sigma-Aldrich) and were then briefly sonicate.[91] Protein extracts were resolved by SDS-polyacrylamide gel electrophoresis (PAGE). Primary antibodies were used at the following dilutions: anti-dPPIL4 (Gp2), 1:3000; anti-Tubulin (DSHB Cat# E7, RRID: AB_528499), 1:10,000; anti-RNA Polymerase II, ARNA-3 (Millipore Cat# CBL221, RRID: AB_2167489), 1:2000; anti-RNA Polymerase II CTD phosphor Ser2 (Abcam Cat# ab5095, RRID: AB_304749), 1:10,000; anti-RNA Polymerase II CTD phosphor Ser5, 4H8 (Abcam Cat# ab5408, RRID: AB_304868), 1:10,000; anti-OGT, H300 (Santa Cruz Biotechnology Cat# sc-32921, RRID: AB_2156938), 1:3000; anti-CUL1 (Thermo Fisher Scientific Cat# 71-8700, RRID: AB_2534002), 1:1000; and anti-Actin (Sigma-Aldrich Cat# A2066, RRID: AB_476693), 1:5000. The band intensity was quantified using ImageJ software (National Institutes of Health, RRID: SCR_003070).

For immunoprecipitation, protein extracts were prepared in modified RIPA lysis buffer (50 mM Tris-HCl, pH 7.5, 150 mM NaCl, 1% NP-40, and 0.25% sodium deoxycholate) and were briefly sonicated. Then, 2 μl of anti-dPPIL4 (Gp1) was added to the extract depending on the target protein, and the mixture was incubated overnight at 4°C with end-over-end rotation. Pre-immune serum was used as a negative control. Finally, 20 μl of Pierce™ Protein A Magnetic Beads (Thermo Fisher Scientific Cat# 88845) was added, and the mixture was further incubated for 3 hours at 4°C with end-over-end rotation. The immune complexes were then eluted from the beads using SDS-PAGE sample buffer.

Immunohistochemistry and confocal imaging

Immunostaining was performed as described previously with minor modifications.[85] Fly heads were cut open, fixed in 2% formaldehyde, and washed with PAXD buffer (1X phosphate-buffered saline, 5% bovine serum albumin, 0.03% sodium deoxycholate, 0.03% Triton X-100.[92] The fixed heads were dissected, and the isolated brains were permeabilized in 1% PBT (1% Triton X-100 in PBS) for 20 min and then blocked in PAXD containing 5% horse serum for 1 hour. Anti-dPPIL4 (Gp1) serum was antigen-affinity purified and used for immunohistochemistry. The following primary antibodies were added directly to the mixtures and incubated for 2 days at 4°C: anti-dPPIL4 (Gp1), 1:700; anti-PDF (DSHB Cat# PDF C7, RRID: AB_760350), 1:200; anti-PER (Rb1),[84] 1:200; anti-TIM (Rb1),[85] 1:200; anti-CLK (Gp2),[86] 1:2000; anti-VRI (Gp2),[7] 1:1000; and anti-NC82 (DSHB Cat# nc82, RRID: AB_2314866), 1:150. The brains were washed with PAXD and incubated overnight with secondary antibodies in a blocking solution at 4°C. The following secondary antibodies were used at a 1:200 dilution: goat anti-rabbit Alexa-488 (Thermo Fisher Scientific, RRID: AB_143165), goat anti-rabbit Alexa-555 (Thermo Fisher Scientific, RRID: AB_2535849), goat anti-guinea pig Alexa-488 (Thermo Fisher Scientific, RRID: AB_2534117), goat anti-mouse Alexa-555 (Thermo Fisher Scientific, RRID: AB_141780), and goat anti-mouse Alexa-633 (Thermo Fisher Scientific, RRID: AB_2535718). Stained brain samples were washed with PAXD, incubated in 0.1 M phosphate buffer containing 50% glycerol for 30 min, and mounted using a mounting medium. Confocal images were obtained using an LSM 800 confocal microscope (Carl Zeiss) and were processed using Zen software (Zen Digital Imaging for Light Microscopy, Carl Zeiss, version 3.1). For signal quantification, the pixel intensity of each cell was determined using ImageJ software. The intensity was recorded as the average of at least six brains for each genotype.

Real-time quantitative reverse transcription-PCR (qRT-PCR)

Total RNA was extracted from fly heads using the QIAzol reagent (QIAGEN). The total RNA (1 μg) was reverse transcribed using an oligo(dT) 20 primer (for mRNA) or a random hexamer primer (for pre-mRNA) and PrimeScript rTase (TaKaRa). Real-time qRT-PCR was performed using a Rotor-Gene 6000 (QIAGEN) device with TB Green Premix Ex Taq (Tli rNase H Plus, TaKaRa). The following primers were used: *dppil4* mRNA forward, 5'-TTAGTAGCTTCGGCGTGCTT-3'; *dppil4* mRNA reverse, 5'-CTTTGAAACGGATTGG GAGA-3'; *per* mRNA forward, 5'-GACCGAATCCCTGCTCAATA-3'; *per* mRNA reverse, 5'-GTGTCATTGGCGGACTTCTT-3'; *per*

pre-mRNA forward, 5'-GTGAGAGCGAGAGCGAGTGT-3'; *per* pre-mRNA reverse, 5'-TATGTAAGCTGCCTGCCCAA-3'. *tim* mRNA forward, 5'-TGATCGAGTTGCAGTGCTTC-3'; *tim* mRNA reverse, 5'-CCCTTATACCCGAGGTGGAT-3'; *tim* pre-mRNA forward, 5'-GTTTCGGTCAGTGTGTGTATCT-3'; *tim* pre-mRNA reverse, 5'-GCTCAACGAACCGCTTACT-3'. Non-cycling mRNA encoding *cbp20* was used to normalize gene expression using the following primers: *cbp20* forward, 5′-GTATAAGAAGACGCCCTGC-3′ and *cbp20* reverse, 5′-TTCACAAATCTCATGGCCG-3′. The data were analyzed using Rotor-Gene Q-Pure Detection software (version 2.2.3), and the relative mRNA levels were quantified using the $2^{-\Delta\Delta Ct}$ method, in which $\Delta\Delta Ct = [(Ct_{(target)} - Ct_{(cbp20)})$ of the experimental group$] - [(Ct_{(target)} - Ct_{(cbp20)})$ of the control group].

PER degradation rate analysis: Cycloheximide (CHX) treatment

To score the degradation rate of PER, *wper*^{01},TUG>*d2*,UAS-*per31* and *wper*^{01},TUG>*d2*,UAS-*per31, dppil4* Ri flies were fed with the protein synthesis inhibitor CHX (Sigma-Aldrich Cat#. C7698) dissolved in sweet food (20% sucrose and 2% agar). Flies were entrained to 12:12 LD cycle at 25°C. On the fourth day under LD conditions, before transferring the flies to the vehicle (ethanol, EtOH) or 5 mM CHX-containing food, flies were starved for 3 hours to promote feeding. The flies were maintained on either vehicle or CHX-containing food, collected at the indicated times, and processed for brain immunostaining for PER.

Feeding assay

To quantify the feeding amount of the flies, the absorbance of ingested dye was measured. Flies were entrained to 12:12 LD cycle at 25°C. On the fourth day under LD conditions, before transferring the flies to the 5 mM CHX-containing food, flies were starved from zeitgeber time (ZT) 21 to ZT0 for 3 hours to promote feeding. At ZT0, the flies were allowed to feed on 20% sucrose and 2% agarose food containing 5mM CHX and 1% blue dye (McCormick). Subsequently, flies were collected at each time point and homogenized in PBS, centrifuged for 3min, and the absorbance of the blue dye in the supernatant was measured at 620nm.

RNA-Sequencing and data analysis

Flies were entrained to 12:12 LD cycle at 25°C. On the fourth day under LD conditions, flies were collected at ZT8 and ZT16. Total RNA from fly heads were extracted using QIAzol reagent (QIAGEN). To assess the integrity of the total RNA, samples are run on the *TapeStation RNA screentape (Agilent, #5067-5576).* Only high-quality RNA preparations, with RIN greater than 7.0, were used for RNA library construction. A library was independently prepared with 1ug of total RNA for each sample by Illumina TruSeq Stranded mRNA Sample Prep Kit (Illumina, Inc., San Diego, CA, USA, #20020595). A library was independently prepared with 1ug of total RNA for each sample by Illumina TruSeq Stranded mRNA Sample Prep Kit (Illumina, Inc., San Diego, CA, USA, #20020595). Indexed libraries were then submitted to an Illumina NovaSeq6000 (Illumina, Inc., San Diego, CA, USA), and the paired-end (2×100 bp) sequencing was performed by the Macrogen Incorporated. The cleaned reads were aligned to the *Drosophila melanogaster* (dm6) using STAR v2.6.0c.[93] The reference genome sequence and gene annotation data were downloaded from NCBI Genome assembly and NCBI RefSeq database respectively. Aligned data (SAM file format) were sorted and indexed using SAMtools v 1.9. After alignment, the transcripts were assembled and quantified using RSEM v1.3.1.[94] Statistical analyses of differential gene expression were performed by DESeq2 v 1.38.[95] using raw counts as input. Filtered data set was applied with RLE normalization to correct the variation of library sizes among samples. Statistical significance of differential expression gene was determined using DESeq2 nbinom WaldTest[95] Fold change and p-value were extracted from the result of WaldTest. All p-values are adjusted by Benjamini-Hochberg algorithm to control false discovery rate (FDR).

DEXseq

DEXSeq (v1.44.0)[96] in R (v4.2.3) was utilized to obtain the exon usage values. Ensembl gene annotations (version 72) were used in the DEXSeq workflow to ensure consistency with the AltAnalyze workflow. Bam files generated by AltAnalyze were used as input for the standard DEXSeq workflow. Since AltAnalyze retains counts for both properly paired and singleton reads, this settings was preserved by setting "fragments = TRUE" when running "*summarizeOverlaps*" from the GenomicAlignments package (v1.34.1).[97]

QUANTIFICATION AND STATISTICAL ANALYSIS

For the statistical analysis, we used Prism9 software (GraphPad by Dotmatics). For comparisons among multiple groups, we used One-way ANOVA followed by Dunnett's multiple comparisons test. To compare two groups, the datasets were assessed for normality using Shapiro-wilk test. If the normality test was passed, we used Student's *t*-test. If the normality test failed, we used Mann-Whitney test. For experiments involving both time series and different genotypes, we used Two-way ANOVA followed by Šidák's multiple comparisons test.